NTNU
Norwegian University of
Science and Technology

Spectroscopic characterization and performance of novel triplet state enhanced molecules for optical power limiting

Didrik Kvanvik Hopen

Master of Science
Submission date: June 2018
Supervisor: Mikael Lindgren, IFY

Norwegian University of Science and Technology
Department of Physics

Abstract

Finding molecules with good optical power limiting (OPL) performance is of great importance for the use in OPL filters made for protecting against harmful lasers used in an expanding set of technologies. In this thesis, the OPL performance and its underlying mechanisms are investigated for three unstudied molecules of so called fluorenes, functionalized to have a triplet state central group. I abbreviate these molecules A, B and C. A previously studied molecule, PtOEP, is also investigated. The results are presented and discussed, in light of the five-level model. The OPL performance of A, B and C is measured with an intensity scanning setup and the results indicate C as the best performer. A large difference in triplet state emission and a forbidden S_0T_1 transition separates C from A and B. This makes triplet reverse saturable absorption (RSA) the OPL mechanism that makes C outperform the other molecules. The contribution of singlet RSA and two photon absorption (TPA) to the OPL performance still have to be further characterized in terms of TPA, in order to obtain a full understanding of the underlying mechanisms. The OPL results are also devalued by the appearance of nonlinear scattering, apparently caused by the formation of small plasma bubbles in the solvent at high fluences.

Sammendrag

Å finne molekyler med god optisk effektbegrensende ytelse er av stor betydning for bruk i OPL-filtre for å beskytte mot skadelig laser brukt i en voksende mengde teknologier. I denne avhandlingen undersøkes den optiske effektbegrensende ytelsen og dens underliggende mekanismer for tre ikke tidligere studerte molekyler av såkalte fluorener, som er funksjonalisert for å ha en sentral triplettilstand gruppe. Jeg tilegner disse navnene A, B og C. Et tidligere studert molekyl, PtOEP, er også undersøkt. Resultatene presenteres og diskuteres, i lys av femnivåmodellen. OPL-ytelsen til A, B og C måles med et intensitetsskanningsoppsett, og resultatene indikerer C til å være molekylet med best ytelse. En stor forskjell i triplettilstand emisjon og en forbudt S_0T_1 overgang skiller C fra A og B. Dette gjør triplet RSA (revers metningsabsorpsjon) til den OPL mekanismen som gir C bedre OPL ytelse i forhold til de andre molekylene. Bidraget fra singlett RSA og TPA (tofotons-absorpsjon) til OPL-ytelsen er i stor grad usortert, og det anbefales å gjøre TPA målinger for å få en mer detaljert beskrivelse av OPL-ytelsen. Verdien til OPL-resultatene blir nedgradert av tilstedeværelsen av ikke-lineær spredning, trolig forårsaket av dannelsen av små plasmabobler i løsningsmidlet ved høye inngangsintensiteter.

Contents

1 Introduction

A laser is a device that emit light through the process of optical amplification based on stimulated emission of electromagnetic radiation. The first laser was built in 1960 by Theodore H. Maiman at Hughes Research Laboratories, based on theoretical work by Charles Hard Townes and Arthur Leonard Schawlow[1]. A laser differs from other sources of light in the way it emits light coherently, spatially and temporally. Spatial coherence allow a laser to be focused to a small spot and a laser beam to stay narrow over great distances, enabling great applications such as laser pointers, lithography, optical communication, fine surgery and laser cutting. However, lasers hold a great potential for harming different optical systems and human tissue such as the human retina. This is is because the spatial coherence enable energy to be focused at very small spot. Where a 50 watt light bulb is harmless, a 50 watt laser (with wavelength in the visible spectrum) focused at the pupil diameter of an eye, will have an intensity 50 000 times the damage threshold of the eye. Lasers are ever-present in the modern day society due to its many uses, therefore, the importance of making good optical filers for the protection of optical systems and the human eye, is crucial.

One of these types of filters are made with molecules limiting incident light non-linearly. This allows incident light to pass at low intensities, while shielding at high intensities. These filters are called passive optical power limiting (OPL) filters.

In the mid 1960s shortly after the invention of the laser, many researchers were investigating dyes for potential application to Q-switching of the laser cavity. For this application, dyes were sought that would bleach to transparency under intense illumination (saturable absorbers). In 1967 Guiliano and Hess[2] were investigating vat dyes and their modified cousins and noted some examples where the molecules did not bleach to transparency, but instead darkened at high intensities. This was the first recognition of the property of reverse saturable absorption (RSA).

RSA and two photon absorption (TPA) are two mechanisms contributing to the passive OPL abilities a material can inhabit. Multiple molecules with high RSA and/or TPA have already been found and some have been successfully implemented in glass[3]. The race to make good filters based on passive OPL protecting against damaging laser radiation based on RSA is well on the way. Also, methods have been developed for anticipating the OPL properties of molecules based on the measurements of a few photophysical properties[3, 4].

In this master's thesis, the passive OPL performance of four molecules are measured with a intensity scanning setup. Via photophysical characterization, the way the three mechanism; TPA, singlet RSA and triplet RSA, affect the OPL performance are investigated. Three of the molecules, molecule A, B and C, have not previously been studied. Their photophysical properties are measured and presented. The photophysical properties of the last molecule (PtOEP) has been studied in detail [5, 6].

The samples of molecule A, B and C were provided by Prof. Chantal Auraud and Prof. Stephane Parola of ENS-Lyon, France, in a joint collaboration project also involving FOI, Sweden. The molecules were syntesized by PhD students Jean-Christophe Mulatier and Adrien Liotta. Futher details are available in their PhD thesis at ENS-Lyon. PhD student Hampus Lundén was responsible for the OPL measurements performed at FOI, Linköping, Sweden, with Didrik assisting in the experiments and data analysis, whereas all photo-physical characterization was carried out in the lab of NTNU.

2 Theory and experiments

2.1 Absorption and luminescense - Background

Luminescence is the emission of photons (light) by a substance that has absorbed photons[7]. Luminescence can be categorized as fluorescence or phosphorescence. In this thesis, the studied substances will be referred to as luminescent substances, consisting of luminescent molecules, regardless of whether they mainly yield both fluorescence or phosphorescence.

Absorption is caused by a molecule obtaining the energy from an incident photon, thus exciting one of the molecules electrons to some excited state, as seen in the Jablonski diagram in figure 1[7]. After a short period of time, the electron loses its energy and gets de-excited to its ground state. There is a variation of de-excitation processes that will yield different outcomes. The energy can be emitted as vibrational energy (heat) or it can be emitted as a photon with slightly lower energy, so called fluorescence. It can also be transferred to a different luminescent molecule or it can be transferred to the triplet state of the same molecule. Three of these processes is illustrated in Figure 1. Here, it is is shown how some of the energy is emitted as heat, as the electron moves from its excited vibrational state, to a lower excited state, in a process called relaxation. The figure also show fluorescence, as the electron moves from the lowest excited singlet state to one of the ground states and phosphorescence, as the electrons moves from an triplet excited state to the ground state. Notice how the electron can cross from the singlet states to the triplet state in a process called inter-system crossing (ISC).

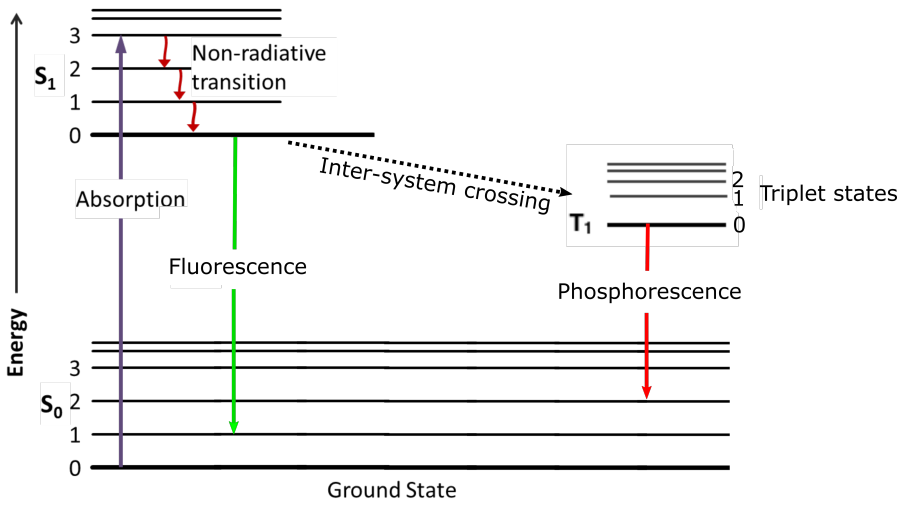

Figure 1: The figure illustrates the different processes that yield luminescence and the processes that yield no radiation in a simple Jablonski diagram. The ground state S_0, the lowest excited singlet state S_1, the lowest triplet state T_1 and their vibrational states (1,2,3,...) can be seen. There are, in reality, more excited and triplet states the electron can be excited to: S_2,S_3,T_2,T_3...

2.1.1 Absorption spectrum

As seen in figure 1, there are multiple, yet a limited set of excited and vibrational states the electron can be excited to. Therefore the different luminescent molecule and solvent combinations

can only absorb light with certain wavelengths λ. The absorbed amount A will vary with the wavelength[7]. This gives us an absorption spectrum as shown in figure 2.

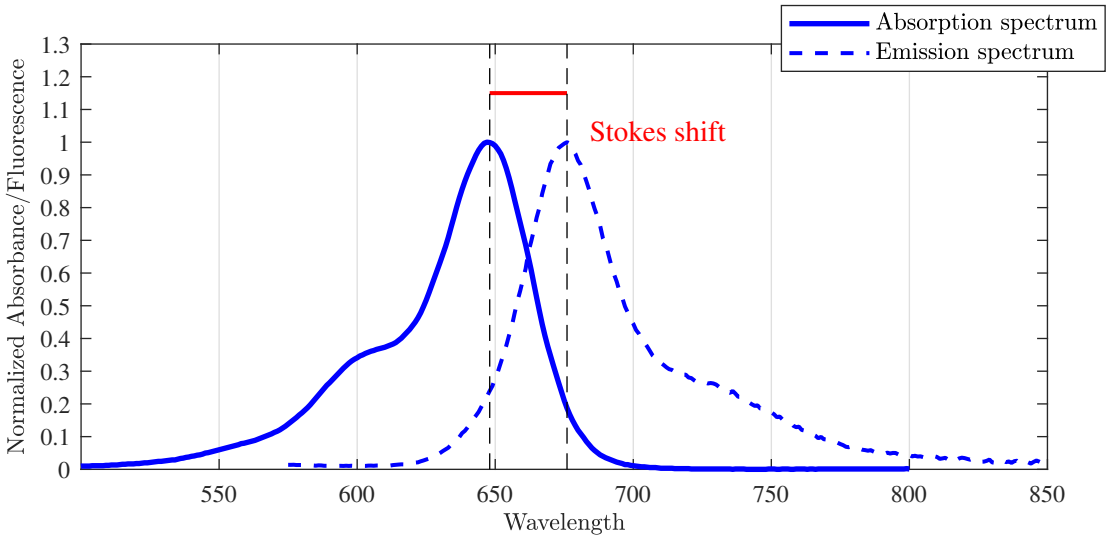

Figure 2: The figure illustrates the absorption spectrum, the emission spectrum and the Stokes shift. In this example, the Stokes shift is found to be 28 nm wide. Wavelength unit is nm.

To determine the absorption potency of a molecular system, the extinction coefficient ϵ [$\mathrm{M}^{-1}\mathrm{cm}^{-1}$] can be determined. ϵ is derived from A in the following way:

$$A(\lambda) = \epsilon \cdot c \cdot l \tag{1}$$

$$\epsilon(\lambda) = \frac{A}{c \cdot l} \tag{2}$$

where c i the concentration of luminescent substance in solvent (given in molars) and l is the length of sample the light passes through[8]. Physically, the absorption A is actually not the amount of absorbed photons by the luminescent substance. A describes how much of the incident intensity that does not pass through the sample. A is the result of absorption, scattering and reflection taken together, unless a background scan is made (see 2.1.5 on page 15). More specifically, A is given by

$$A(\lambda) = \log_{10}(\frac{I_i}{I_t}) = \log_{10}(T), \tag{3}$$

where I_i is the intensity of the incoming light, I_t is the intensity of the transmitted light and T is the transmittance of the material[8].

Ground state absorption spectrometer

A Hitachi U-3010 spectrometer was used for the ground state absorption (GSA) measurements in this project. As seen in figure 3, the U-3010 uses a reference vial filled with solvent in addition to the sample vial filled with both dye and solvent. The beam from the illumination source

is split into two equal beams using a beam splitter, before they pass through their designated vials. The intensities of the beams, having passed through the vials, are recorded and used as I_i and I_t in formula 3. Using the intensity of a beam having passed through a sample as I_i, as opposed to the actual incident beam, removes the effects of scattering and reflections of the solvent. All of these calculations are handled by U-3010's software.

Scattering due to impurities in the sample vial can also be corrected for by doing a measurement with only solvent, before the dye is added. The correction for this "baseline" is handled by U-3010's software.

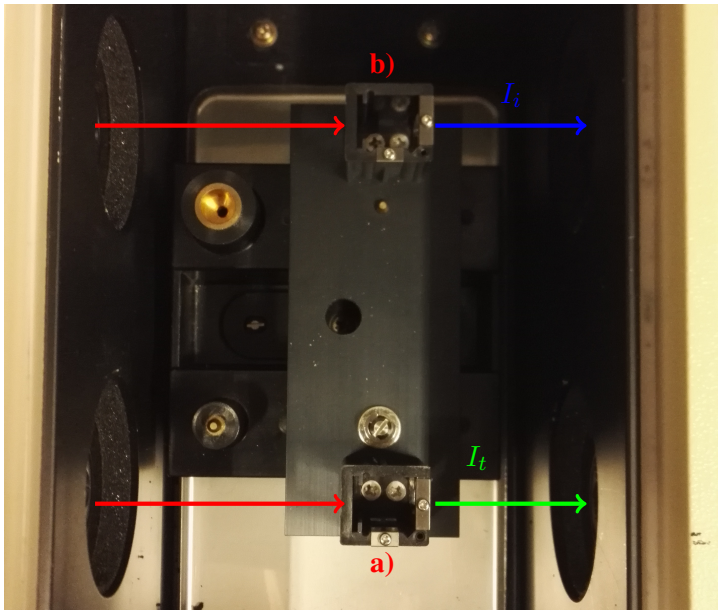

Figure 3: Shows the vial holders and the beam paths in the Hitachi U-3010 spectrometer. a) is the sample vial holder and b) is the reference vial holder. The red arrows illustrates the two equal beams, before they interact with the reference and sample. I_i and I_t illustrates the beam path after the interactions.

As reported by the manufactures, its wavelength range is $190\,\mathrm{nm}$ to $900\,\mathrm{nm}$, its wavelength accuracy is $\pm 0.3\,\mathrm{nm}$ and the accuracy of the absorbance is set to be $\pm 0.004\,\mathrm{Abs}$[9]. Abs is the measurement unit described as A in formula3. The Abs values used in typical measurement are in the range of $0\,01$ to $2\,\mathrm{Abs}$.

2.1.2 Emission spectrum

Because of energy lost in the relaxation processes the luminescence will have an equal or longer wavelength than any absorbed light. If a luminescent substance absorbs light of a particular wavelength, it will emit light with a range of different energies. These energies will vary because the different luminescent substances have different excited states, and this gives a specific emission spectrum for a specific luminescent substance. The emission spectrum is generally presented as a plot of the luminescence intensity versus wavelength.

The maximum of the emission spectrum will have a longer wavelength than that of the maximum of the absorbed spectrum. The distance between these two maxima is called the Stokes shift[7]. How large the Stokes shift is, and what the emission spectrum will look like, will vary between different luminescent substances. An example of an absorption and emission spectrum pair, and its Stokes shift, is shown in figure 2.

To obtain an emission spectrum, light with a specific wavelength can be used to excite the molecular system. This wavelength is called the excitation wavelength. The emitted spectrum will, in general, only contain wavelengths longer than the excitation wavelength. This, however, does not make emission spectrum shape dependent of the excitation wavelength[7]. Using a too high excitation wavelength will merely cut off the spectrum. Also, the use of different excitation wavelengths will result in different emission spectrum sizes. Using excitation wavelengths that the luminescent substance of interest absorbs more of, will result in more emission.

As explained in section 2.1 on page 9, the luminescence of the emission spectrum can mainly be separated into fluorescence and phosphorescence. Dependent on the luminescent molecule in study, the emission spectrum will consist either only fluorescence, only phosphorescence or a mix of the two. In spectra where the molecules emit both, the fluorescence and the phosphorescence will often be separated into different parts of the spectrum. Either in different parts in the same curve or as two different curves (as can be seen in figure 25 on page 34).

Emission spectrometer apparatus

In this thesis, the PTI QuantaMaster^{TM} 8000 spectrometer was used for the emission measurements. As seen in figure 4, the 8000 sends light with a specific excitation wavelength to the sample vial. The luminescence will be emitted in all directions. The excitation light that did not get absorbed passes straight through the sample vial. Measurements are made on luminescence coming from an orthogonal angle relative to the incident light.

Background scans (see section 2.1.5 on page 15) with the 8000 is made by doing a measurement with only solvent, before the dye is added.

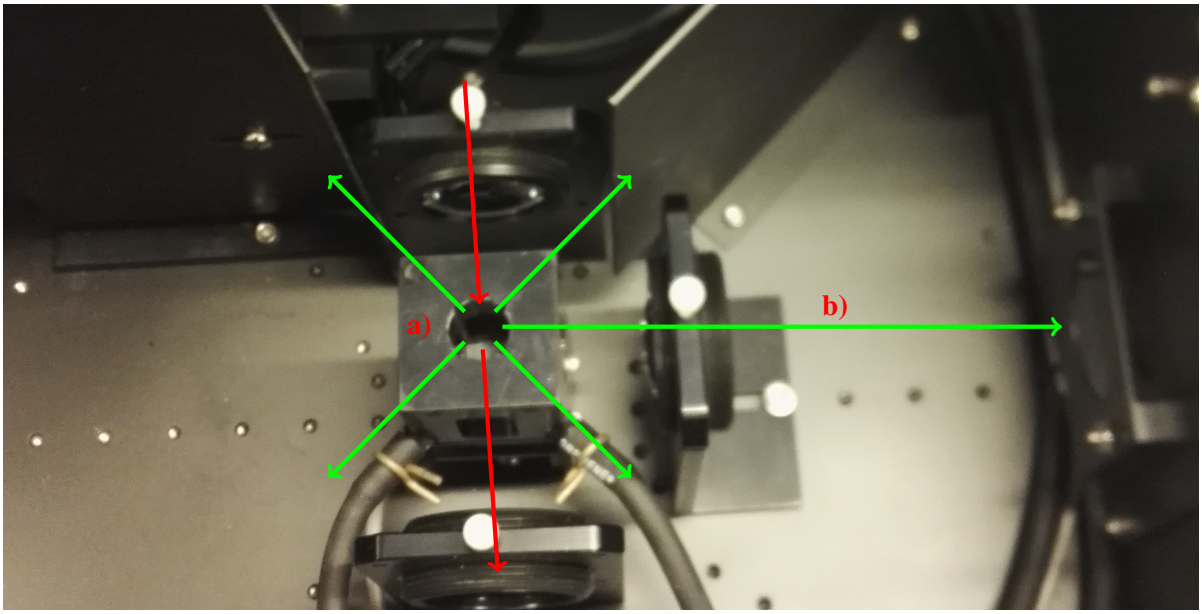

Figure 4: Shows the vial holders and the beam paths in the PTI QuantaMaster^{TM} 8000 spectrometer. The red arrows indicate the path of the incident beam and the part of the beam that did not interfere with the sample. The green arrows indicate the luminescence beam paths (all directions). a) is the sample vial holder and b) is the parts of the path of the emitted beams that passes on through to the detector.

As reported by the manufactures, its wavelength range is $185\,\mathrm{nm}$ to $900\,\mathrm{nm}$, its wavelength accuracy is $\pm 0.3\,\mathrm{nm}$ and the signal to noise ratio is $30'000:1$[10]. For emission measurement

over $900\,\mathrm{nm}$ a liquid nitrogen cooled detector had to be used.

2.1.3 Excitation spectrum

A excitation spectrum looks a lot like an absorption spectrum. In the same way as a an absorption spectrum is measured, the sample under investigation is excited with the range of wavelengths of interest. The difference is that instead of looking at the change of intensity caused by absorption, the luminescence of a specific wavelength is measured.

This is done in the same PTI QuantaMaster^{TM} 8000 spectrometer used for measuring the emission spectum. As seen in figure 4, the sample in position a) is exposed to incident along the directions of the red arrows. In the pathway of the luminescence b) a monochromator sorts out the wavelength of interest, before the signal is measured by a detector. As seen in figure 5, the excitation spectrum represents the intensity measured by the wavelength of the light that was exciting the sample at the specific time. Even do the excitation spectrum looks a lot like the absorption spectrum (as seen in the same figure), different absorption wavelengths contribute to the emission of different wavelength luminescence.

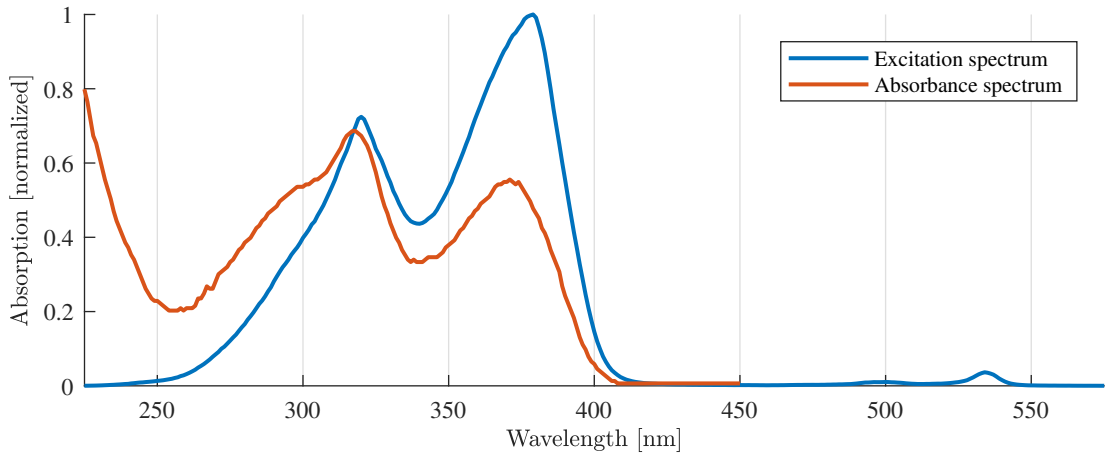

Figure 5: The figure shows the plotted data for a GSA spectrum and a excitation spectrum measured at a specific wavelength.

2.1.4 Lifetime

The period of time the excited electron stays in an excited state before it is de-excited is called the fluorescence or phosphorescence lifetime. Different luminescent substances will have different lifetimes, but the fluorescence lifetime is usually found to be between 10^{-12} and 10^{-8} seconds[7].

Due to quantum mechanical selection rules, an electron in a triplet state has a smaller statistical chance of moving to the ground state. This gives the phosphorescence a much longer lifetime than fluorescence, and can normally be found to be between 10^{-6} and 10^{0} seconds[7].

In this thesis, the fluorescent lifetime, the phosphorescence lifetime and the excited state absorption (ESA) lifetime is measured. Measuring these lifetimes is done by exciting the luminescent

substance multiple times with a laser pulse or a flash, and measuring the time it takes for the sample to get de-excited and reach some detector. The detector samples light with specified wavelength. So that the lifetime of different parts of an emission spectrum can be measured separately.

Because of the short lifetime of the fluorescent emission, a prompt measurement representing the response time of the system has to be made with a substance with known lifetime. The technique used in the flourescent lifetime measurement is TCSPC (time correlated single photon counter). For this technique, a single laser pulse excites the sample, then the lifetime of the first few photons reaching the detector is averaged and sampled in a histogram. This process is repeated until a preset amount of counts is measured, resulting in an histogram as seen in the histogram in figure 6. The prompt is also shown in the figure.

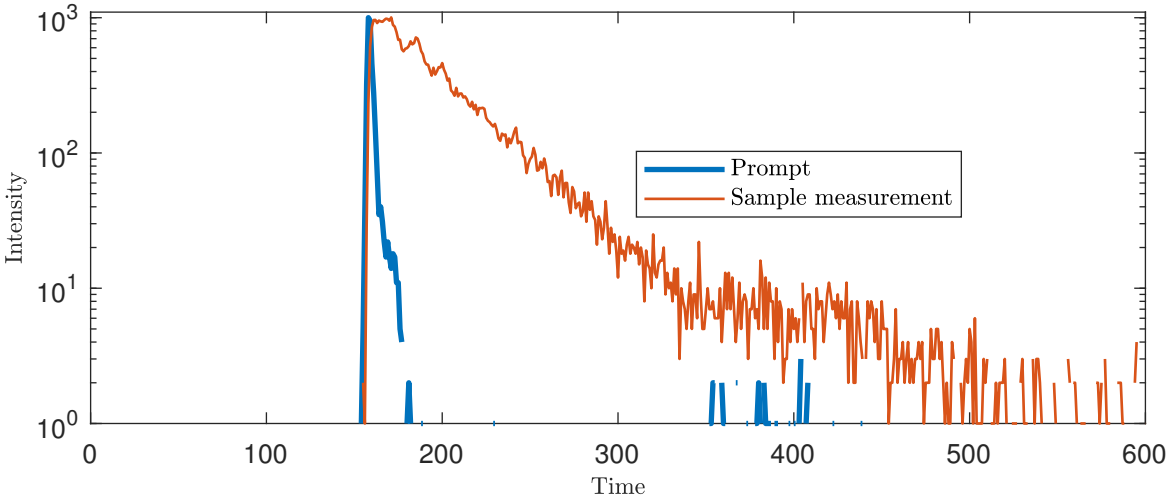

Figure 6: The figure display a TCSPC lifetime measurement.

The measuring process of phosphorescence lifetime differs some from the fluorescence lifetime measuring process and the technique used is called MCS (multi-channel scaling). The phosphorescence lifetime does not require any prompt because of the long lifetimes. The detector consist of multiple channels staying open for a specified time interval ($0\,5$-$500\,\mu s$), at a specific times after the sample is excited. The next channel opens when the previous channel closes. This process is repeated for multiple flashes, until a specific amount of counts is reached.

Measuring the ESA lifetime is done in about the same manner as the phosphorescence lifetime was made in. The difference lies in the way the luminescent substance is excited. The ESA lifetime measured is the time an electron, excited from an already excited triplet state, stays in that higher triplet state. See section 11 on page 20 for further details about ESA.

As seen in figure 6, sorting the data on logarithmic scale, a straight line seems to appear. The lifetime τ can be calculated from the following formula:

$$I(t) = I_0 e^{-t/\tau},$$

given that the data only consists of one lifetime[7]. $I(t)$ is the intensity at time t and I_0 is a constant calculated from the data. If multiple lifetimes happen to be measured at the same time, computer software calculate the lifetimes.

2.1.5 Background scans

When a luminescent substance is under investigation, the interest lies in the photophysical properties of the substance, as well as how it is affected by the solvent. What is not interesting, is the absorption and emission coming from the solvent itself. These attributions can be removed by acquiring the solvent spectrum and subtracting it from the spectrum of the solution. The solvent spectra are called background scans. These scans also remove other unwanted affects from the luminescent substance spectra, such as scattering due to impurities in the sample vials, additional signal from unwanted reflections and background noise from the apparatus.

2.1.6 Cross-sections

Cross sections (σ) is a more detailed way of describing the different sorts of absorption measurements presented above. As seen in figure 1, an electron can be in multiple states. In a microscopic view, the probability of the electron moving from one state to another varies with the population of the state and the incident intensity.

In a macroscopic view, this transition probability is called the cross-section of the transition. As the transitions occur at different timescales, the different cross-sections are also dependent on the duration of exposure to light[4]. A laser pulse may for example give a different cross-section, than a continuous wave (CW) give for the same transition, even if both the pulse and the CW have the same intensity. However, this is only the case if the pulse width and the transition time is in the same scale.

The transition from the singlet ground state to any other state (measured by the absorption spectrum apparatus 2.1.1) is called the GSA cross section. This cross-section σ is proportional to the extinction coefficient ϵ in equation 2 in the following way:

$$\sigma(\lambda) = \frac{\ln 10 \cdot 1000 \frac{\mathrm{cm}^3}{\mathrm{dm}^3}}{N_A} \cdot \epsilon(\lambda), \tag{4}$$

where N_A is Avogadros number[4].

2.1.7 Sample preparation

The fluorescent substances used in this project came in powder form and had to be dissolved in a solvent. A small amount ($\sim \mathrm{mg}$) of the dye was measured out using a micro balance weight and mixed with some solvent ($\sim \mathrm{ml}$) to get a stock solution of approximately $0.5\,\mu\mathrm{g/ml}$[1]. The stock solutions were meant to be used as a basis for multiple measurements.

To do measurements on the dyes with the apparatuses, the stock solution had to be diluted to achieve a sample concentration of about $2.5 \times 10^{-3}\,\mu\mathrm{g/ml}$[1]. A low enough concentration to avoid self quenching (see section 2.1.8 on the next page, but high enough to produce clear aborption/emission. The sample was mixed in a standard vial (see figure 7) made for usage in all apparatuses except for the intensity scanning setup (see section 2.2.3 on page 22).

[1]The chosen concentrations were based on advises from the supervisor.

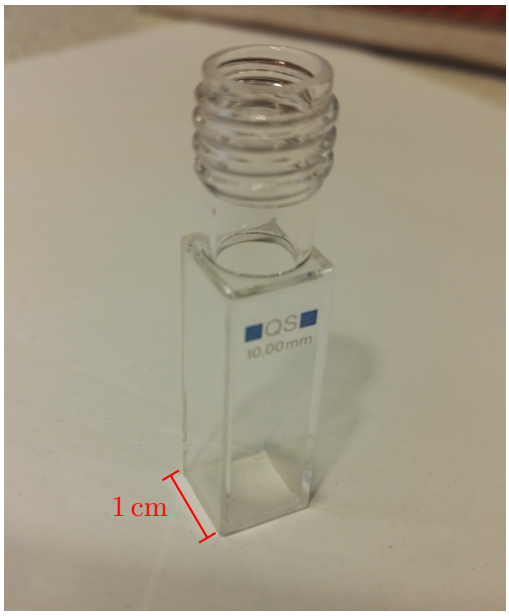

Figure 7: The picture shows the sample vial used for all measurements, except the intensity scanning. The length any beam passes through the sample in such measurements is visualized.

2.1.8 Quenching

Luminescence quenching refers to any process which decreases the luminescence of a given substance. A variety of processes can result in quenching. Some of these processes, called self quenching processes, require molecular contact between two luminescent molecules[11], where one of the molecules are excited. This sort of quenching will therefore depend on the concentration of solution, as well as diffusion and excitation lifetime. Self quenching does, however, not affect the shape of the absorption spectrum[11]. Another type of quenching is oxygen quenching. The cause of the quenching is that the ground state of oxygen (O_2) is a triplet state and that it therefore easily can interact with triplets states of other molecules by collision, making the triplet state of the luminescent molecule decay faster[4]. Since the phosphorescence lifetime is so long, the statistical chance of oxygen removing most of the phosphorescence of a luminescent molecule is large, if oxygen is present. Therefore, to measure the phosphorescence of any soluted luminescent molecule, with solvent containing oxygen, the oxygen has to be removed from the solution.

2.1.9 Deoxygenation technique

Non-water based organic solvents like tetrahydrofuran (THF) is often used to dissolve solute that water based solvents can not solute. These solvents dissolve a lot of oxygen from the ever-present air and has to be removed with a deoxygenation technique to avoid oxygen quenching[12]. To remove the oxygen in these the measurements of this thesis, the solution was bubbled with argon for eight minutes. To bubble the solution, a rubber cap was used on the standard vial shown in figure 7. A syringe needle penetrating the cap ejects argon at the bottom of the vial. A second syringe is set up to let the oxygen out at top of the vial. As argon is heavier than oxygen it will replace and push any oxygen to top of the vial, where it can escape through the second syringe.

2.1.10 Quantum yield

The quantum yield (QY) is the emitted number of photons per the absorbed amount of photons[13]. This is an important photophysical factor, as it says something about the efficiency of the luminescent substance in study[7]. Different luminescent substances will have different QY values. If the luminescent substance is dissolved in a solvent, the QY will vary with different concentrations. However, the QY will have the same maximum value for all concentrations below a certain concentration. At too high concentrations the QY will fall because of self quenching (see section 2.1.8 on the previous page).

Method for finding the QY

To find the QY of a luminescent substance the absorption and emission spectra of different concentrations in dilute are measured. The absorption values at the excitation wavelength used in the emission spectra is found and the integrals of the emission measurements are found. By plotting these two values with different solution concentrations, and using linear regression, a straight line can be found (see figure 9 as an example). The gradient of this line is proportional to the QY of the substance of interest.

By repeating this procedure on a luminescent substance with a known QY value (a reference) and using the following formula:

$$QY = QY_{ref} \cdot \frac{\eta^2}{{\eta_{ref}}^2} \cdot \frac{a}{a_{ref}}, \tag{5}$$

the desired QY can be found[11]. Where QY_{ref} is the QY of the reference substance, η and η_{ref} are the refractive indices of the dilutes and a and a_{ref} are the calculated gradients.

A important requirement for the use of this method is that the measurements of the luminescent substance and the reference has to be made with the same apparatus settings and excitation wavelength[13]. Combining this criteria and what is written in section 2.1.2 on page 11, two requirements for the reference comes to light:

- The absorption spectrum of the reference needs to overlap the absorption spectrum of the luminescent substance i question.
- The excitation wavelength can not overlap the emission spectrum of either the studied substance or the reference.

An example of a reference meeting these requirements is shown in figure 8.

To find the QY, as explained in 2.1.10, multiple measurements with different dye concentrations had to be made. To achieve this, $750\,\mu l$ of the sample was replaced with dilute, before new measurements were made. This procedure was repeated until 3 emission and absorption measurements were made. In the instances where these three measurements did not align in an emission integral/absorbance plot due to self quenching (see example in figure 9), the procedure was repeated until the concentration was low enough to produce at least four aligned measurements.

The integral of the emission spectrum was calculated, with the data produced by the emission spectrometer apparatus. The absorption was extracted directly from the data produced by the

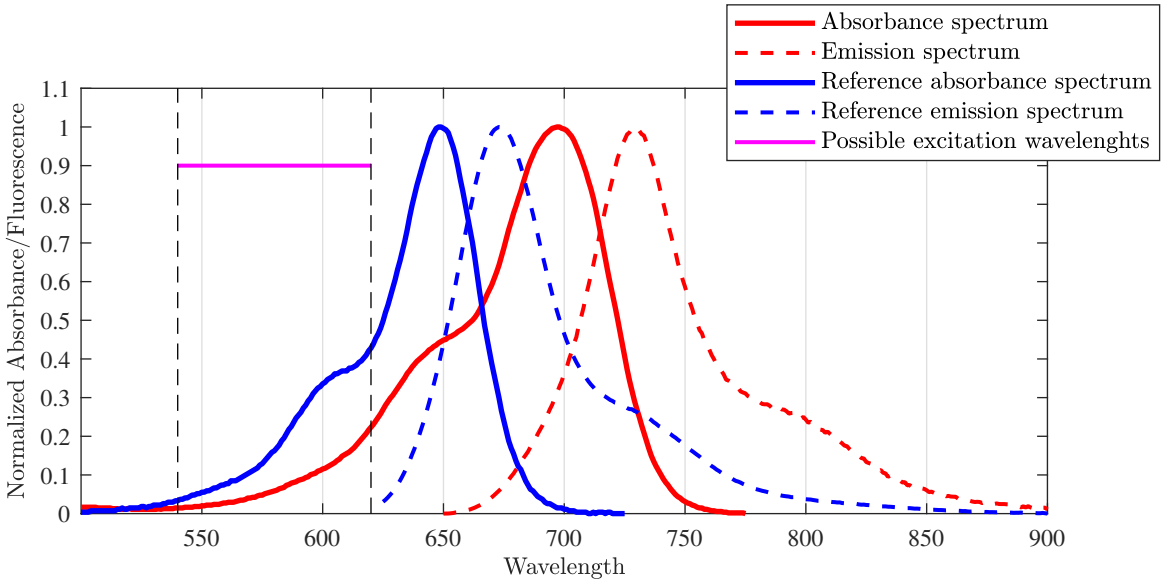

Figure 8: The figure illustrates the relations between the different spectra and possible excitation wavelengths in measurements made to calculate the QY of a dye-dilute combination. Notice how there would be no possible excitation wavelengths, if the reference emission spectrum had started at a wavelength lower than $540\,\mathrm{nm}$. Wavelength unit is nm. The Y-axis unit is luminescence and not fluorescence.

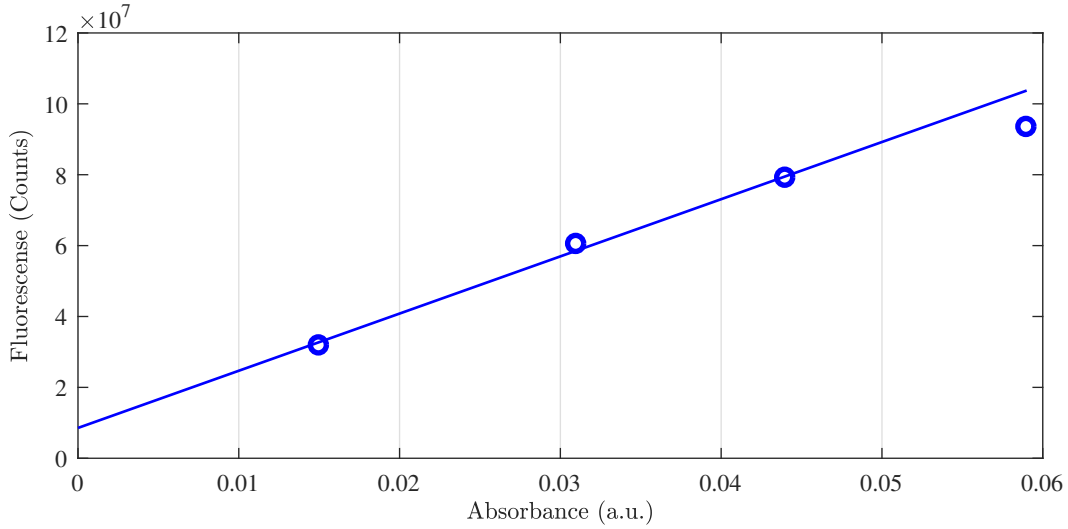

Figure 9: This plot visualizes the linear correlation between luminescence and absorbance. The measurement in the upward right corner does not align (most probably) due to quenching. The Y-axis unit is luminescence and not fluorescence.

absorption spectrometer apparatus. The gradient of the line (and its uncertainty) seen in the emission integral/absorbance plot (that was used to calculate the QY), was found using least square linear regression.

The first absorption measurement conducted in the process of finding the QY, was also used to produce the extinction coefficient spectrum. To obtain this spectrum, the absorption spectrum was only divided by the molar mass of the sample, as the width of vial used in the measurements

is exactly $1\,\mathrm{cm}$ (see figure 7). The molar mass was calculated from the noted concentrations and the molecular weight of the dye. Note that the absorption measurements may be used even if self quenching was present, as self quenching does not affect the shape of the absorption spectrum.

2.2 Optical power limiting

There are a wide range of optical power limiting (OPL) methods, but they can broadly be categorized into two different types; dynamic and passive OPL[14]. With dynamic OPL, a photosensor controls some sort of iris that restricts the intensity of light incident on an optical system. There are virtually an infinite number of schemes and devices that can be constructed to control light in such a manner. With passive OPL, the material is self-activated and limits damaging laser radiation by a photophysical mechanism.

Dynamic OPL is superior to passive in many ways, due to obvious reasons. Passive OPL is, however, faster, more size-practical and possibly more affordable, as dynamic OPL generally depends on a sensor, processor and actuation module[14].

One type of passive OPL is based on the photophysical phenomenon of nonlinear absorption (NLA). NLA means that the absorption of the OPL material increases exponentially in relation to increase of incident light. Passive OPL can also arise from nonlinear scattering and nonlinear refraction. However, because of practical optical design reasons discussed by Lundén et.al.[3], NLA as the dominant mechanism is preferable to avoid a fraction of the refracted/scattered radiation being recollected in a optical system.

2.2.1 Reverse saturable absorption

A molecule with reverse saturable absorption (RSA) is a molecule whose excited state absorption (ESA) cross section is larger than the GSA cross section[14]. The opposite ratio will result in a molecule with saturable absorption (SA). RSA contributes to a molecules OPL performance.

The OPL effect of RSA can be explained by the five level model[14][3]. This model, illustrated in figure 10, is dependent on the transition cross sections between, and the lifetimes of, five of the states an electron can be in. The inter-system crossing times between are also a part of the model.

Some luminescent molecules with RSA does only need to be explained by the three singlet states in the five level model (se figure 10). If $\sigma_{S_1S_2}$ is larger than $\sigma_{S_0S_1}$, the NLA will rise as S_1 gets populated and $\sigma_{S_1S_2}$ starts contributing to the total absorption cross section. This is only valid for very intense and/or short laser pulses (sub nanoseconds[14]) as $\tau_{S_1S_0}$ and $\tau_{S_2S_1}$ usually are very short (ns).

If there is a large enough of inter-system crossing ISC this will contribute to the RSA in the same matter a large $\sigma_{S_1S_2}$ does. However, $\tau_{T_1S_0}$ is usually very long ($\mu\mathrm{s}$) and any incident laser pulse can therefore be longer and/or less intense in proportion to the length of $\tau_{T_1S_0}$.

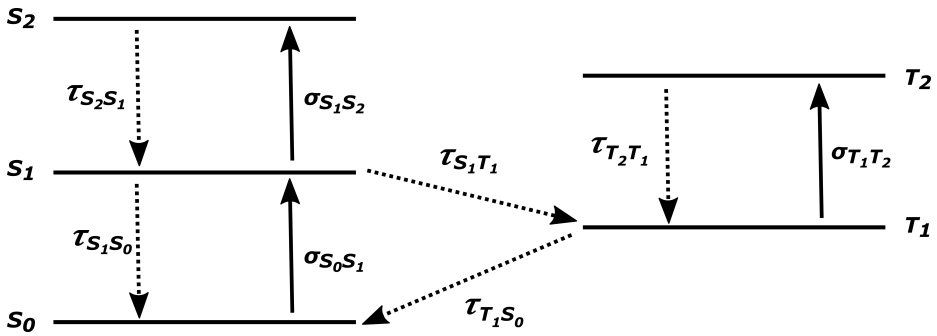

Figure 10: The figure illustrates the five level model. The three lowest singlet states S_N, the two lowest triplet states T_N, the cross sections between the states σ, the lifetimes of the states τ and the inter-system crossing lifetimes τ are visualized.

Excited state absorption (ESA) measurement setup

The following setup operates with flashlamps with $\sim$ µs flash lengths. Therefore, the ESA spectra produced by this setup only represent the triplet T_1T_N part of ESA (triplet ESA) and not S_1S_N (singlet ESA).

As illustrated in figure 11, a pump flashlamp excites as many of the luminescent molecules of the sample from the ground state to some excited state. Straight thereafter ($\sim$ µs), while the pump flashlamp is still operating, the probe flashlamp further excites the sample. The delay between the two flashlamps is controlled by the delay box. In the pathway of the probe flashlamp, after the sample, a optical multichannel analyzer (OMA) samples the light having passed through the sample to produce an absorption spectrum as seen in figure 12.

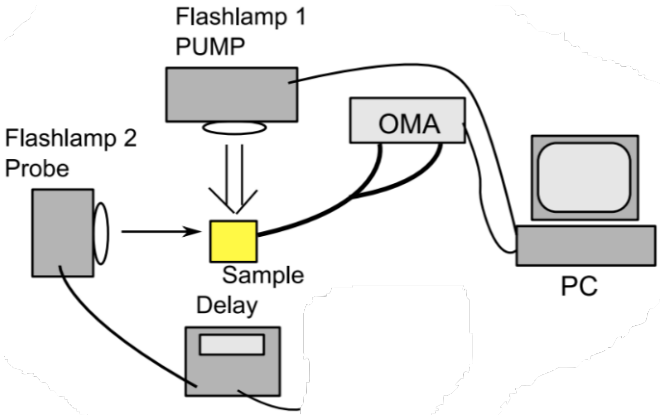

Figure 11: The figure illustrates the main parts of the ESA measurements setup. Notice the orthogonal beam paths of the PUMP flashlamp and the Probe flashlamp.[4]

However, this absorption spectrum made by the OMA does not represent the ESA spectrum, as a fraction of the luminescence produced by the pump flashlamp is measured by the OMA, resulting in the "negative" absorption of figure 12. To correct the absorption spectrum, a percentage of the absorption spectrum made on the same sample can be added. The percentage will be the same as the percentage of molecules excited by the pump flashlamp[4]. This percentage is not known, but has to be guessed by trying to add different percentages of the absorption spectrum and looking at what seems sensible in regards to removing "negative" absorption and in relationship to the alignment of the spectrum at the edges of the addition range[4, 15]. The addition of an absorption spectrum and a correct ESA spectrum is shown in figure 13.

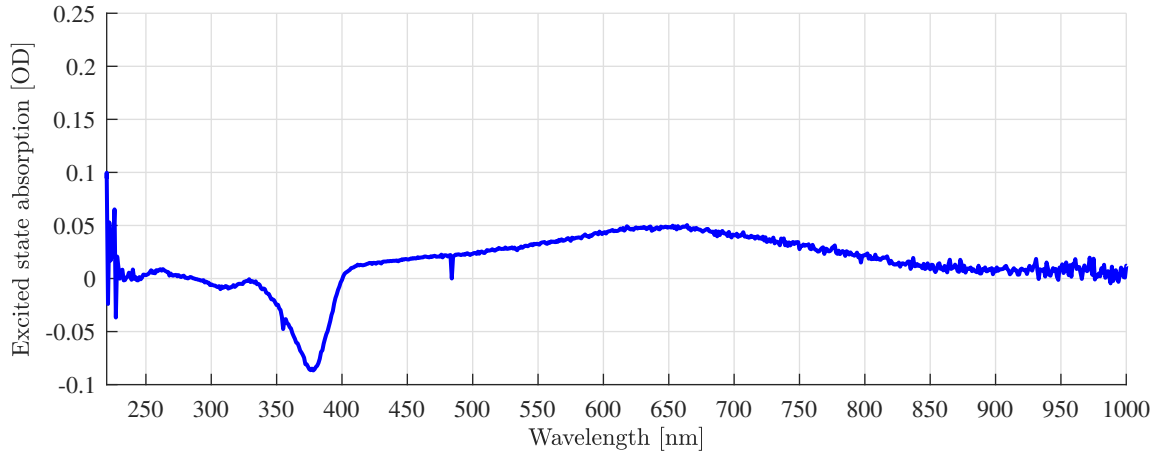

Figure 12: The figure displays an example of what is measured by the OMA. Notice how the absorption is "negative" from 300 nm to 400 nm.

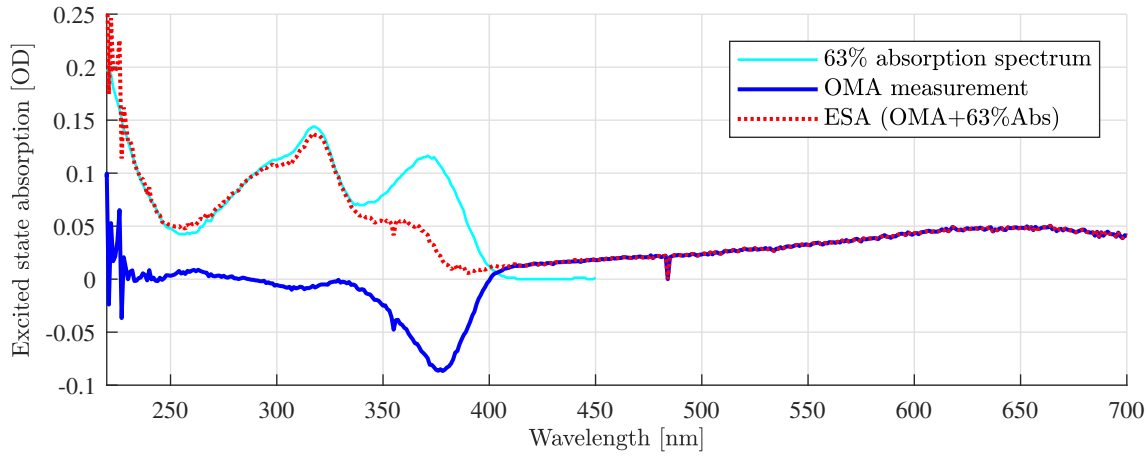

Figure 13: The figure displays what is measured by the OMA, 63% of the GSA spectrum and the corrected ESA spectrum. Notice how the OMA spectrum goes from "negative" to positive, as the 63% absorption spectrum is added.

The delay box offers to change the delay between the two flashlamps to find the delay that produces the maximal absorption. The delay was tested between zero and 60 µs. All the ESA spectrum measurements were made with deoxygenated tetrahydrofuran (THF) as solvent as the absorption to triplets states are measured.

2.2.2 Two photon absorption

Two photon absorption (TPA) is a phenomenon that occurs if an electron is excited via photon absorption to an intermediate virtual state and straight thereafter is anew excited to a real state. The probability that a second photon is at the right place at the right time increases non-linearly as the incident beam intensity rises[3]. TPA only contribute to the NLA of a molecule for high intensity nanosecond pulses[3]. Three photon absorption, four photon absorption and so on, can also occur, yielding the same nonlinear effect. However, in this thesis they will all be referred to as the same effect, TPA.

2.2.3 Measuring NLA with intensity scanning

There are multiple techniques for evaluating the nonlinear performance of OPL materials[16]. One of the most used techniques is the intensity scanning method (usually made with an $f/5$ setup). In this sort of measurement, the intensity on incident light on the sample is varied. The nonlinear (or linear) change in the intensity of the light that has passed through the sample is measured. This is done for multiple wavelengths. An example of how the data is presented is shown in figure 14. As can be seen in the figure, the data is often presented by input fluence ($\mathrm{J/cm^2}$) versus output energy (µJ). The data can also be seen as aligning in two linear areas, the first (aprox. $< 3\,\mathrm{J/cm^2}$) and the second(aprox. $> 8\,\mathrm{J/cm^2}$), with a nonlinear area between. There are not actually two strictly linear areas, but for practical reasons, the OPL data is split up in this manner.

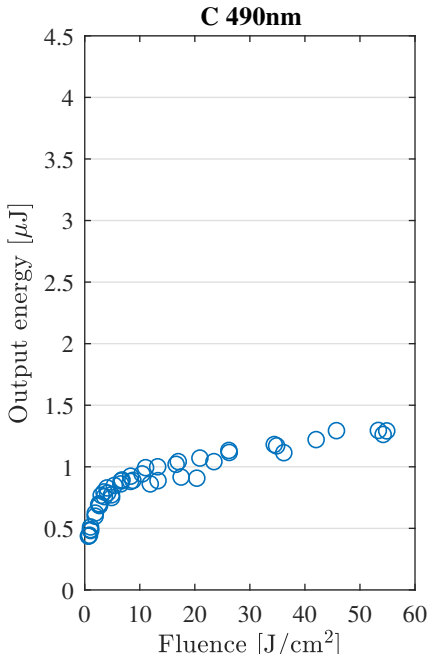

Figure 14: The figure illustrates the plotted OPL data for the luminescent molecule C. The wavelength of the incident light was $490\,\mathrm{nm}$

Intensity scanning setup

A figure of a intensity scan setup can be seen in figure 15. A EKSPLA NT-342C laser sends out $\sim 0 - 80\,\mu\mathrm{J} \sim \mathrm{ns}$ pulses. In the path between the controlling mirrors (M in fig. 15), there is a beam cleanup setup (not seen in fig. 15) to shape the beam into a top hat shaped collimated $2\,\mathrm{cm}$ diameter pulse. These pulses are recorded by an Ophir PE9-C reference detector (D1 in fig. 15).

Thereafter, the beam is sent through a f/5 x2.5 magnification system. Inside this system, the sample (S in fig. 15) is placed in the common focus of lens L1 and L2 (see fig. 15). It is important to ensure that the beam is spherical at the sample position. The size of the spot ($\sim 10^{-7}\mathrm{cm^2}$) has to be measured to calculate the input fluence. The sample width is only $2\,\mathrm{mm}$ to ensure that sample is only occupying focused space.

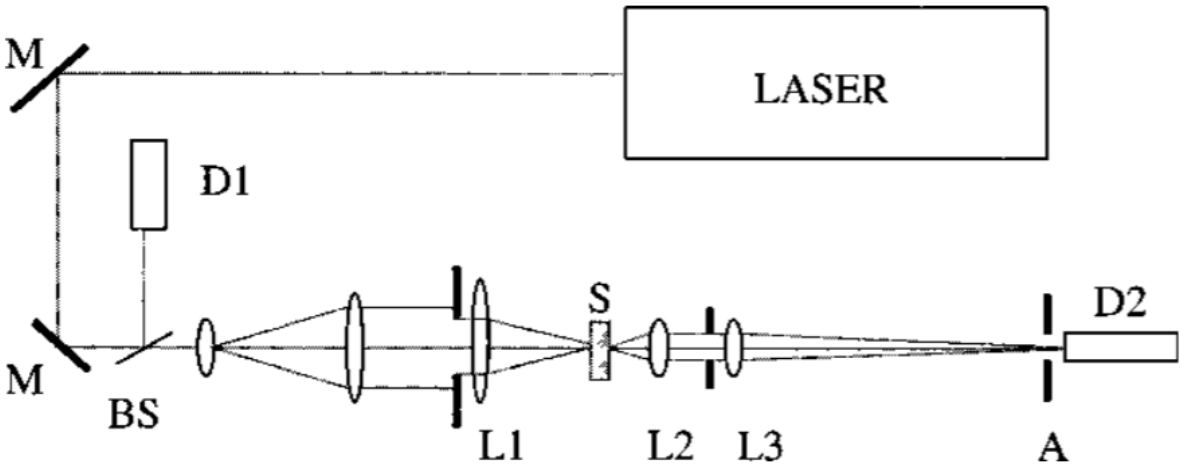

Figure 15: The figure illustrates a intensity scanning setup. The beam path and the elements manipulating the beam is shown. This includes the mirrors M, the beams splitter BS, the lenses L1-L3 and the apertures A.. The position of the sample S, the reference detector D1, the signal detector D2 and the laser (LASER) can be seen.[17]

A pinhole (A in fig. 15) is placed in front of the PD10-C signal detector (D2 in fig. 15) to remove scattered light at high fluences[17]. The size of the aperture is in proportions to the theoretical beam width. By making a few measurements in the first linear area (see the left side of figure 14) both with and without the aperture, the OPL contribution from nonlinear scattering and nonlinear refraction can be visualized.

The solvent used in the OPL measurements is dichloromethane (CH_2Cl_2) in opposition to tetrahydrofuran (THF) that was used in all other measurements. This is because the intensity scanning need high concentrations of the luminescent substance ($25\,\mathrm{mM}$), and THF did not sufficiently dissolve the luminescent substance.

As described by James and McEwan, if a carbon based solution is sufficiently heated by ns to $\mu\mathrm{s}$ pulses, a bubble of microplasma can be created[18]. These microplasma bubbles have nonlinear OPL effects caused by nonlinear scattering. Another result found by James and McEwan, is that different solutions has different threshold input fluences for the production of the microplasma bubbles.

2.2.4 Predicting good OPL performance

As well as explaining RSA, the five level model can be used to predict the RSA and TPA of a molecule and its potential contribution to the molecules OPL performance[3, 4, 19]. Eirik Glimsdal and Hampus Lundén et. al have done this by making models with setups with many commonalities to the intensity scan setup used in this thesis, with regards to beam intensity, pulse length and so on[3, 4]. The photophysical properties related to the TPA, singlet RSA and triplet RSA was manipulated to give indications of how they affected the OPL performance measured by for example a intensity scanning setup.

To make such predictions, the following photophysical properties of interest: The absorption cross section $\sigma_{S_0S_1}$, the cross section of the forbidden transition from the ground state to the lowest triplet state $\sigma_{S_0T_1}$, the triplet absorption cross section $\sigma_{T_1T_N}$, the TPA absorption cross section ω_S, the inter-system crossing (ISC) lifetime $\tau_{S_1T_N}$, the phosphorescence lifetime $\tau_{T_1S_0}$

and the fluorescence lifetime $\tau_{S_1S_0}$[3].

$\sigma_{T_1T_N}$ is very important as it is very closely linked to the triplet RSA. $\sigma_{T_1T_N}$ is derived from:

$$\Delta A(\lambda, t) = A(\lambda, t) - Ag(\lambda) = (\epsilon_T(\lambda) - \epsilon_g(\lambda)) \cdot C_T \cdot L,$$

where ΔA is the ESA spectrum seen in figure 13 on page 21, A is the OMA measurement seen in figure 12 on page 21, A_g is the GSA, C_T is the concentration of molecules in the excited state and L is the sample length[4]. By rearranging this equation and combining it with equation 6, $\sigma_{T_1T_N}$ can be calculated as:

$$\sigma_{T_1T_N}(\lambda) = \frac{\ln 10 \cdot 1000 \frac{\mathrm{cm}^3}{\mathrm{dm}^3}}{N_A} \cdot (\frac{\Delta A(\lambda)}{C_T \cdot L} + \epsilon_g). \tag{6}$$

Glimsdal explains that high $\sigma_{T_1T_N}$ values (a triplet RSA mechanism) are the most important factor for high OPL performance. Triplet RSA can be improved by having higher absorption from the ground state to triplet state. Either by singlet GSA $\sigma_{S_0T_1}$ with inter-system crossing or by direct forbidden transition $\sigma_{S_0T_1}$. The first is dependent on having a high inter-system crossing percentage. Two additional factors contributing to the OPL performance in setups with short pulses is explained by Lundén. The ISC crossing time have to be short enough to populate T_1 fast enough to absorb the start of the pulse and the phosphorescence lifetime have to be long enough to keep the electrons in a triplet state as long as the incident beam passes.

By the viewing the modeling where TPA is the only factor contributing to the OPL performance, Glimsdal explain that the TPA cross section ω_S has to be close to record breaking, to produce OPL in the magnitudes of triplet RSA by it self. However, large TPA can contribute to substantial OPL performace and even be the dominant mechanism. TPA can also contribute to the population of the triplet states, and increase RSA, very effectively.

2.2.5 OPL molecules used in laser protection

One of the ways to utilize OPL molecules is by the use as laser protection filters for optical systems. To show how well a OPL molecule protects against damage, the incident intensity (energy or fluence) that will damage the optical system, has to be defined as the damage energy. The duration of the exposure to incident light will effect this number, depending on the optical system. Is it a short pulse, long pulse or continuous wave? An eye has, as an example, a damage threshold of $0.2\,\mu\mathrm{J}$ (or $0.5\,\mu\mathrm{J}/\mathrm{cm}^2$) for pulses shorter than $17\,\mathrm{ms}$[20]. An minimal accepted percentage of transmission of light where the protection filter is not protecting the optical system, has to be defined. In the visible spectrum, 40% can be used as a rule of thumb, even though this depends on the optical system that is under protection[20]. The concentration of molecules integrated in the filter is an important factor, as higher concentrations protects better. An example of highly concentrated OPL molecules in glass, is $400\,\mathrm{mM}$ in a silica hybrid sol–gel material [21].

For a laser protection filter, the ratio of transmitted energy to maximum incident energy in terms of orders of magnitude protection OD_{sys} (optical density) is defined as:

$$OD_{sys} = -\log_{10}(\frac{E_t}{E_{dam}}), \tag{7}$$

where E_t is the pulse energy transmitted to the sensor, and E_{dam} is the failure threshold of the protective device. In general, for optical systems involving the human eye, an OD of 4 is preferred as the desirable maximum protection[20]. The dynamic range (the ratio of the input energy at which the device fails to the input energy at which it begins to protects) has to be in the same or a higher magnitude as the OD_{sys}[20]. So, OD_{sys} should be ≥ 4 for an eye.

2.2.6 The investigated molecules

The photophysical properties of PtOEP are well investigated. It is a platinum complexed porphyrin, with the molar mass of $787.84\ \frac{\mathrm{g}}{\mathrm{mol}}$. Further information can be found in the articles of Bansal et.al and Nifiatis et.al[5, 6].

A, B and C are three equally constructed platinum complexes, where the difference lies in the addition of two Br groups for B and two PBu_3 groups for C. The molar masses are $2225\ \frac{\mathrm{g}}{\mathrm{mol}}$, $2383\ \frac{\mathrm{g}}{\mathrm{mol}}$ and $2797\ \frac{\mathrm{g}}{\mathrm{mol}}$, respectively. No further information was given.

3 Results and discussion

3.1 Deoxygenation

The argon bubbling technique described in section 2.1.9 on page 16 clearly works as a considerable rise in phosphorescence can be seen post bubbling (see figure 25-27), but how well does it remove the oxygen? The technique is shortly described by Glimsdal. Glimsdal[4] explain that oxygen start to diffuse back after the bubbling has stopped, and that this limits the time span and consistency of consecutive measurements.

To make an estimate of how well the oxygen was removed with this setup in relation to other setups, phosphorescence lifetime data of PtOEP in deoxygenated THF was aquired from a article by Bansal et.al.[5]. Comparing that lifetime ($50 \pm 20\,\mu s$) with the lifetime measured in this thesis ($77 \pm 0.09\,\mu s$), an indication of how well the argon bubbling technique removes oxygen is given. This is possible because in the phosphorescence process the lifetime increases in proportion with how much of the oxygen is removed. The technique used in this thesis seems to be more efficient than the technique used by Bansal et.al. (the technique used by Bansal et.al. is not described in the article).

3.2 Nonlinear scattering

As laid out in section 2.2.3 on page 22, measurements was made with and without a pinhole to figure out whether nonlinear scattering and nonlinear refraction was present. These measurements were made in the first linear area of the OPL plots, and no difference was found for any wavelength or molecule.

The reason why only a few measurement without pinhole was made in the first linear range, was to save time, as doing the intensity scanning measurements was a lengthy process. However, this should be a large enough range as nonlinear scattering and refraction should (by the nature of their mechanism) effect the measurement at any input fluence, in opposition to nonlinear absorption that only occur above a specific input fluence.

With a few of the OPL measurements, the whole input fluence range was measured both with and without pinhole. See figure 16 as an example. As seen in this figure, the open and closed data match well in the first linear range, excluding the influence of nonlinear scattering and refraction. The mismatch between open and closed data in the higher input fluence is therefore caused by some other mechanism. The mechanism is probably scattering caused by the creation of bubbles of microplasma due to heating of the sample at high input influences.

This obviously deteriorates the value of the OPL data, but how and to what degree this does change the output energy at high fluences? As one of the proposed uses for these OPL molecules is glass-integration, it is interesting to ask the question of whether more or less NLA would have been present if there were no creation of microplasma bubbles.

The first point is that if the light had not been scattered by the bubbles, this light would have contributed to higher output energies in OPL measurements without microplasma bubbles. How much higher depends on how well these microplasma bubbles scatter in terms of angular offset from the beam path. Another point, potentially estimating more NLA in glass samples, is

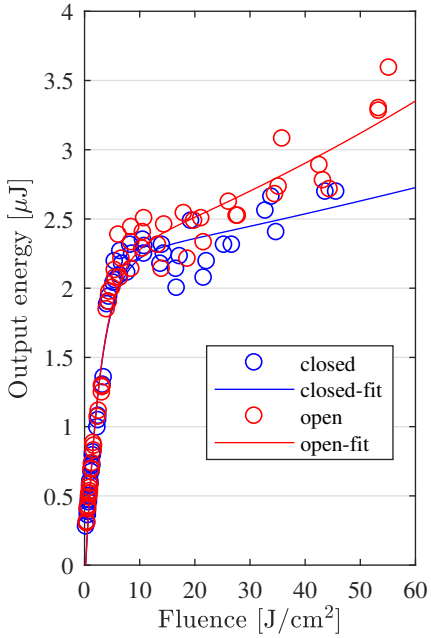

Figure 16: The figure illustrates the OPL data, with and without a pinhole in front of the detector, of molecule A with incident light of 525 nm. The fitting of the data is also shown.

whether microplasma bubbles in carbon based solvents may reduce absorption as parts of the solvent changes its state to plasma.

These points were found hard to investigate, so for further studies, tests on glass samples can sort out the microplasma bubble issue. The use of another solvent, with a higher input fluence threshold for the production of microplasma bubbles, could also solve the challenges.

3.3 Detector issues

As can be seen in figure 17 in all of the OPL plots, there seems to be clustering of the data plots. This is caused by limiting energy ranges of the PD10-C signal detector used in the intensity scanning setup. The detectors energy measurement range had to be changed multiple times during one round of measurements.

If one draws a line along the first linear part of the OPL data plots, not only are there jumps in the direction along the line, but the plots also seem to be moving in the orthogonal direction of the line. This is caused by over- and/or undermeasurement of the signal in the outer parts of the signal ranges.

3.4 Using a filter to measure full emission spectrum of molecule C

When one measures the emission of a luminescent substance having luminescence in wide range of wavelengths, a problem with second order harmonic diffraction (SOHD) may occur. In the emission apparatus, SOHD is caused by the grating that selects which wavelength that is sent to the detector. As seen in figure 18 at approximately 330 nm-420 nm and 660 nm-840 nm, at double the wavelength of any measured emission, noise will appear. This poses a problem, as

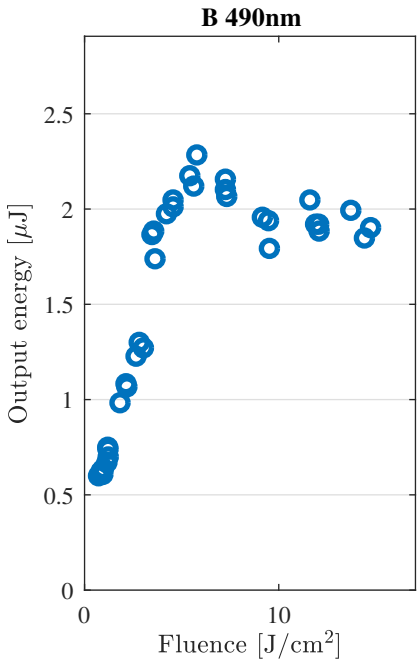

Figure 17: The figure shows a zoomed in version of figure 49 in the appendix.

the correct emission spectrum is not shown and the value of the integrated spectrum will be wrong.

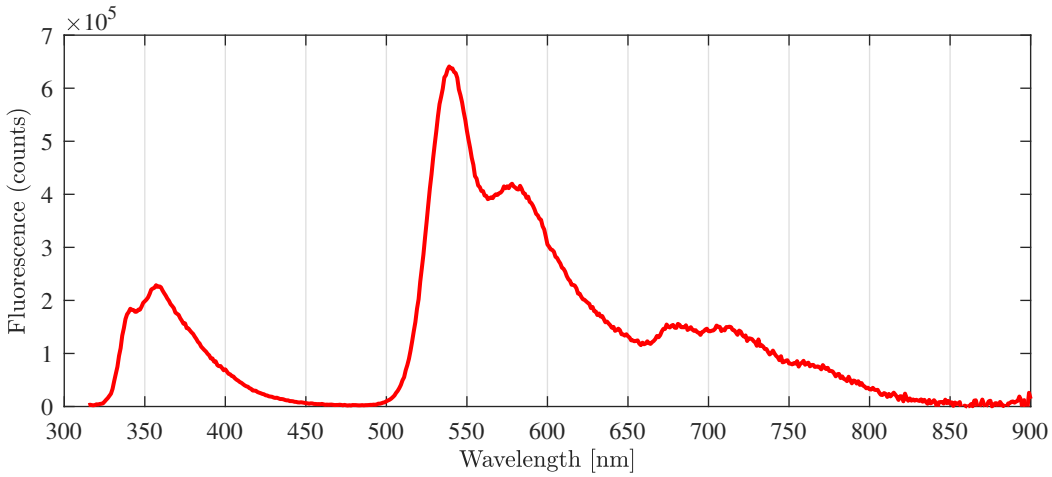

Figure 18: The figure shows the emission spectrum of the molecule C. SOHD can be seen around 660 nm-840 nm.

A 450 nm longpass filter placed in position b) of figure 4 removes the noise caused by SOHD, as can be seen in figure 19. To produce a complete and noise free version of the emission spectrum, the first part of the no-filter spectrum was combined with the filter spectrum. To account for the reduced transmission above the cut-off wavelength caused by the installed filter (see the height difference in figure 19) the filter spectrum was multiplied with

$$\frac{\int_{500\,\mathrm{nm}}^{625\,\mathrm{nm}} S(\lambda)d\lambda}{\int_{500\,\mathrm{nm}}^{625\,\mathrm{nm}} S(\lambda)_{filter}(\lambda)d\lambda},$$

where S is the no-filter spectrum function and $S(\lambda)_{filter}$ is the filter spectrum function.

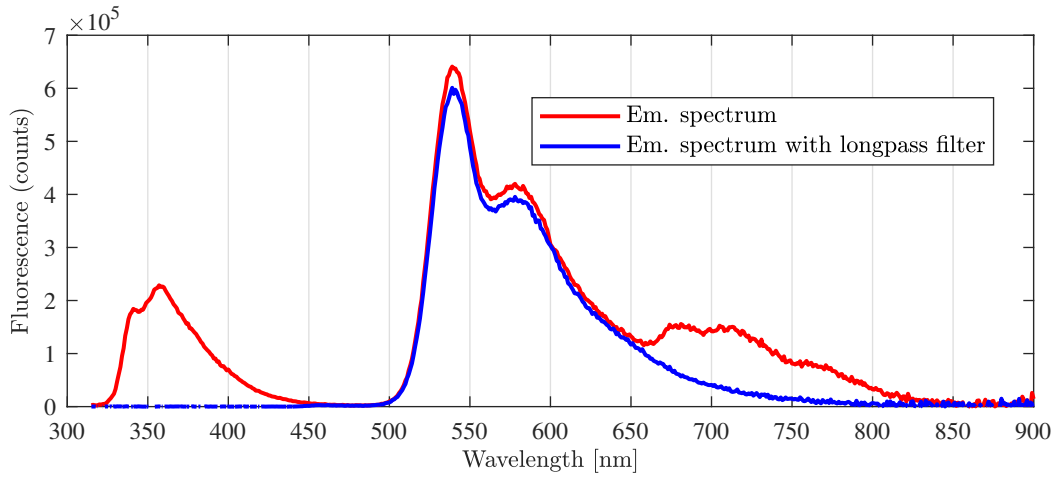

Figure 19: The figure shows the emission spectrum of the molecule C, with (blue) and without (red) a longpass filter. SOHD can be seen around 660 nm-840 nm.

3.5 An hypothetical example of OPL molecules in laser protection

Looking at what specifications is needed to estimate how well an molecule might work as a power limiting filter in (as described in section 2.2.5 on page 24), the molecule C will be investigated.

Lets say that an optical system is being exposed to a short $450\,\mathrm{nm}$ laser pulse. The pulse is shaped as a near top-hat shape collimated $1\,\mathrm{cm}$ diameter beam. The maximum transmitted energy E_t for the optical system is $0.1\,\mathrm{J}$ and the input area of the optical system is $1\,\mathrm{cm}^2$. The requirement set for the protection filter is that the dynamic range and optical density is ≥ 2.5.

Even though the OPL data sets seem to be somewhat off the actual values due to bubble scattering (see section 3.2 on page 27), in this hypothetical example the OPL performance will be said to follow the fitted curve of figure 20. The protection filter in this example is made of a $2\,\mathrm{mm}$ glass, with a concentration of $400\,\mathrm{mM}$, resulting in an increased OPL performance of $\frac{400\,\mathrm{mM}}{25\,\mathrm{mM}}$, in comparison to the OPL data of figure 20. The beam used in the intensity scanning apparatus was focused into a $\sim 5 \cdot 10^{-7}\mathrm{cm}^2$ spot. As this system may be exposed to a $1\,\mathrm{cm}^2$ spot, and no other optical lenses are present as part of the protection filter, the output energy would be $\frac{1}{5 \cdot 10^{-7}}$ times the output energy in comparison to the OPL data of figure 20.

Given these specifications, what input intensity can the system with the OPL filter withhold, what is the actual dynamic range and what is the optical density? The OPL of the imagined glass sample exposed to a $1\,\mathrm{cm}^2$ beam and the input signal in relation to the output damage threshold is illustrated in figure 21. From this curve we can read that the damage threshold of the system (E_{dam}) is about $37\,\mathrm{J}$. Equation 7 on page 24 gives us an optical density of $-\log\frac{0.1}{37} = 2.57$ and there is a dynamic range of ≥ 2.57 orders of magnitude.

The fit of the data in figure 20 and 21 does not cross origo, which is unnatural, as zero fluence should yield zero output energy. The reason for this may be attributed to the detector jumps described in section 3.3 on page 28 and to few measurements being made at low input fluences.

In this imagined hypothetical situation, using the OPL plot of molecule C as if it represents the actual power limiting abilities, the C molecule works well. As the real OPL performance probably is a bit lower (see section 3.2), the filter would have had a lower dynamic range

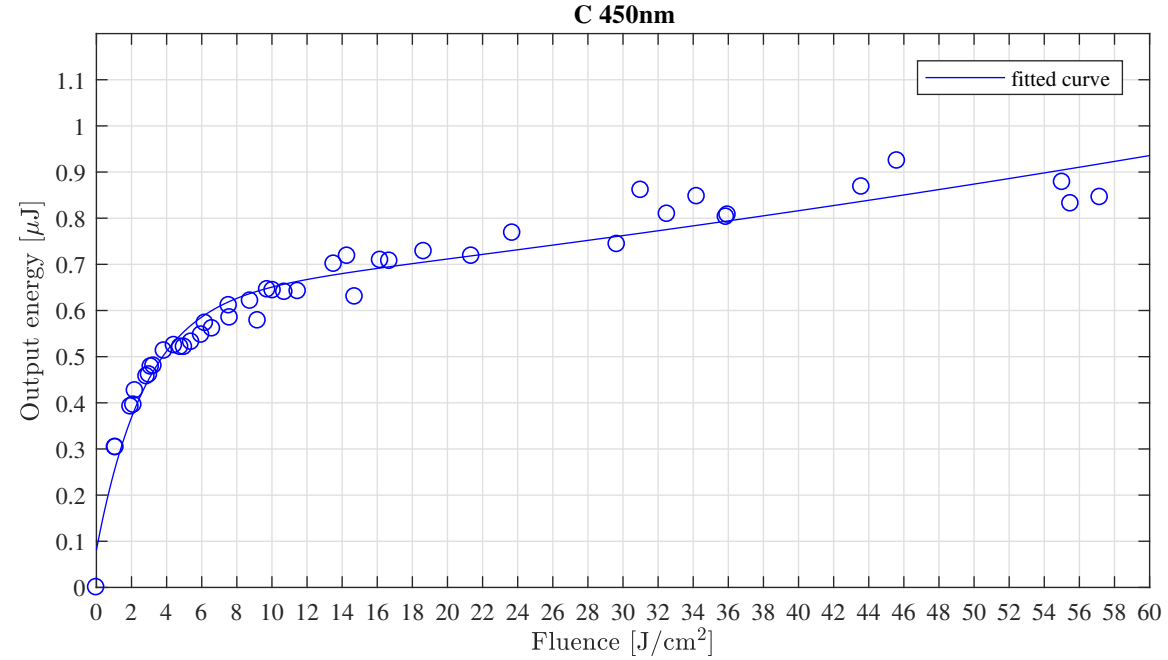

Figure 20: In this figure the OPL data of molecule C with incident 450 nm light is shown. A fitted curve is also shown.

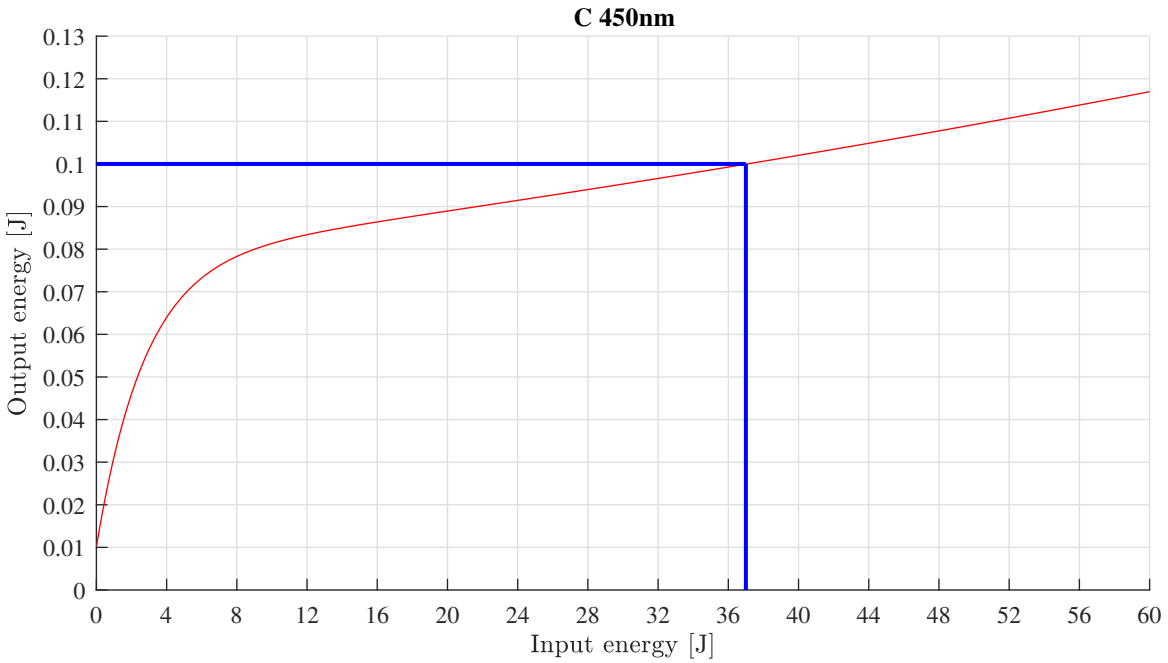

Figure 21: The figure illustrates the same fitted curve as in figure 20, only that the output energy is $\frac{25}{400}$ the size. The damage threshold E_{dam} and the maximal transmitted energy E_t of the imaginary system is visualized by two blue lines.

and optical density. However, implementing a focusing mechanism, changing the concentration and/or changing the glass thickness could change the NLA to a desired level. In other situations, protecting against different wavelengths or pulse lengths, its performance would vary.

As seen in figure 34 on page 40, all three molecules have a varying degree of the nonlinear effect at different wavelengths. Testing the different molecules in the same way as C, could give some grounds for comparing the relative OPL performance. Two natural variables to observe, as

the different molecules are exposed to the same situation, would be the E_{dam} and the optical density(OD)/dynamic range, but as the graphs are nonlinear, E_{dam} might occur in the first linear area. This both enlightens the importance for having a good enough molecule for your filter needs and it also indicates that fixing E_{dam}=37 J and looking at the change in E_t would serve looking at the performance of nonlinear effect better, as 37 J is in the second linear area for all molecules and wavelengths (see OPL data in section B on page 48 in the appendix). So, for an $450\,\mathrm{nm}$ incident beam, the maximal transmitted energy (E_t) would have to be $0.3\,\mathrm{J}$ for A and $0.26\,\mathrm{J}$ for B, resulting in an OD of 2.09 and 2.15, respectively.

As seen from the results in figure 34 on page 40, the intensity scanning measurements were only performed on the molecules A, B and C. No measurements on PtOEP was made, as CH_2Cl_2 did not dissolve the substance.

3.6 The different photophysical measurements

The GSA extinction coefficient spectra of the four molecules is presented in figure 22. They were derived from the measured absorption spectra and the sample concentrations. What can be read from the spectra is the similarities between A, B and C, having relatively similar absorption ranges and extinction coefficients. This is understandable as they all are very similar platinum complexes. However, PtOEP does have two distinctly different absorption ranges. The ranges λ_{abs} and absorption peaks λ_{max} can be found in table 1.

Molecule[a]	Extinction coefficient[b] $\epsilon[\mathrm{cm}^{-1}\mathrm{M}^{-1}]$	$\lambda_{max}[\mathrm{nm}]$[c]	$\lambda_{abs}[\mathrm{nm}]$[c]
A	$3.2 \cdot 10^6$	321	250[d]- 397
B	$2.9 \cdot 10^6$	323	250[d]- 376
C	$1.7 \cdot 10^6$	317 (371)	250[d]- 408
PtOEP	$1.4 \cdot 10^4$	380 (534) (501)	250[d]- 445 (478 - 546)

[a] All the molecules were soluted in tetrahydrofuran(THF). [b] These are the exctinction coeffients used in figure 22 on the next page. [c] Secondary ranges or peaks are presented in parenthesis. [d] $250\,\mathrm{nm}$ is chosen as start absorption wavelength, as most transparent luminescent substances starts to absorb a lot at lower wavelengths.

Table 1: The table contains GSA coefficient data.

In figures 23-27 the plotted emission spectra of the molecules can be found, comparing the emission with and without deoxygenated solvent. What can be seen from all the spectra is an increase in luminescence if the solvent has been deoxygenated. The increase in luminescence can also be seen by the increase in QY in table 2.

The shape of molecule A and B stay the same for both solvents, and there is a luminescence increase of 6 and 88 percent, respectively. With C, deoxygenation results in an additional emission range, increasing the luminescence by 850 percent. As with A and B, the shape of PtOEP stay the same (see both figure 26 and 27), while there is an increase in luminescence of 350'000 percent, which indicates that nearly all excited electrons occupy the triplet states. This corresponds well with a previous study of PtOEP, suggesting a near 100% inter-system crossing lifetime $\sigma_{S_1T_N}$[5].

Another point regarding the exctinction coefficient spectrum of PtOEP is its small size. Even if the OPL performance is very good in terms of high nonlinear absorption, in comparison

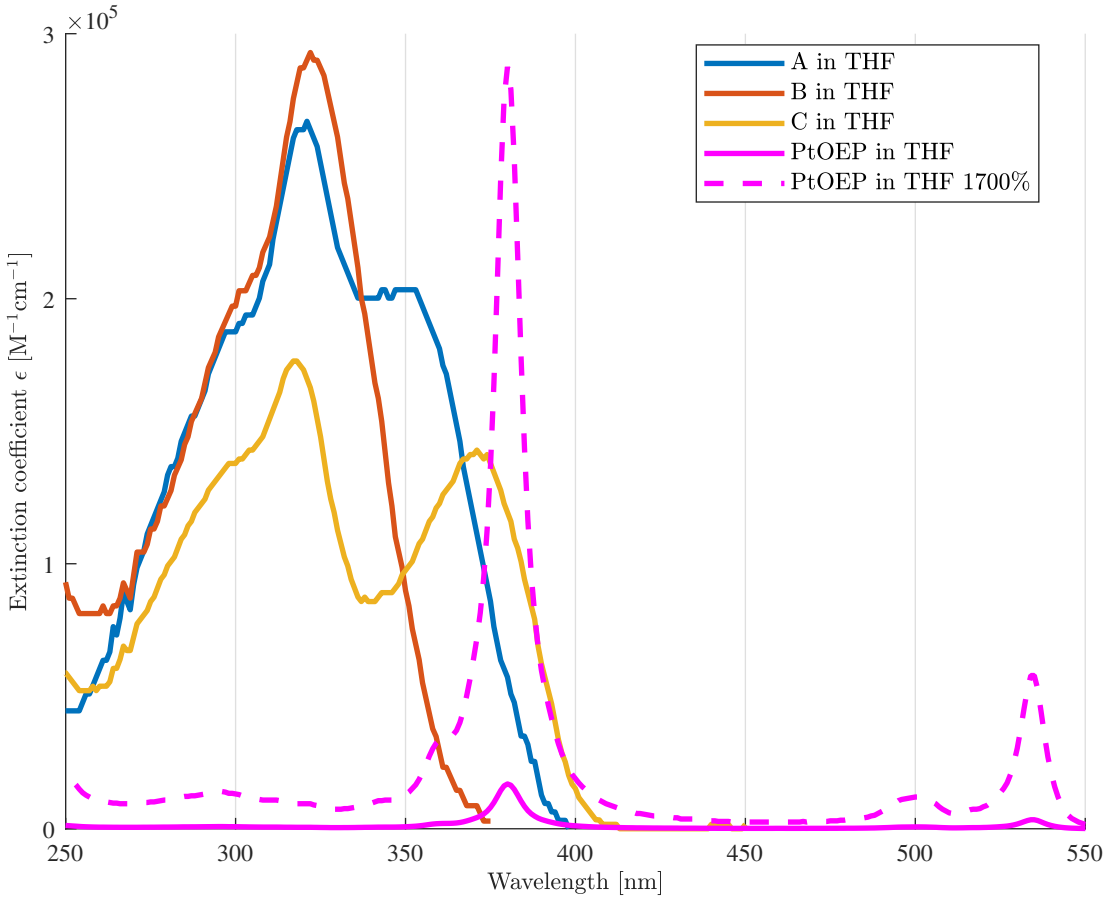

Figure 22: The figure illustates the GSA exctinction coefficient spectrum in a plot. The extinction coefficients are listed in table 1 on the preceding page. A 17x version of PtOEP is also plotted to visualize its shape more clearly.

with A, B and C, the concentration of PtEOP would have to be much higher to achieve similar absorption. This may be a problem for certain applications, as the usable concentrations for some uses may be limited. As an example, the glass samples detailed in section 2.2.5 on page 24 have a limited possible concentration. However, the molar mass of PtOEP is about a third of A, B and C molar mass, and may affect possible concentrations.

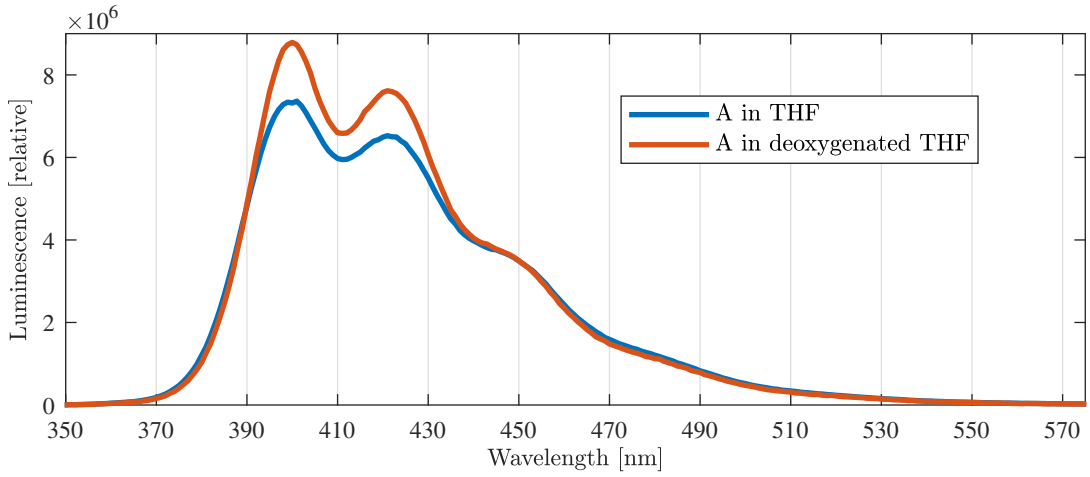

Figure 23: The figure illustates the emission spectrum of molecule A in THF and deoxygenated THF.

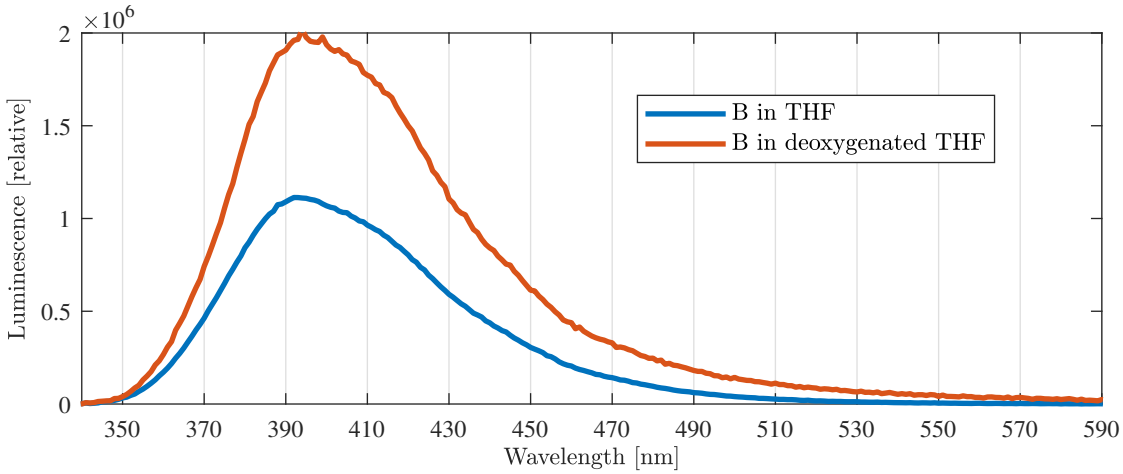

Figure 24: The figure illustates the emission spectrum of molecule B in THF and deoxygenated THF.

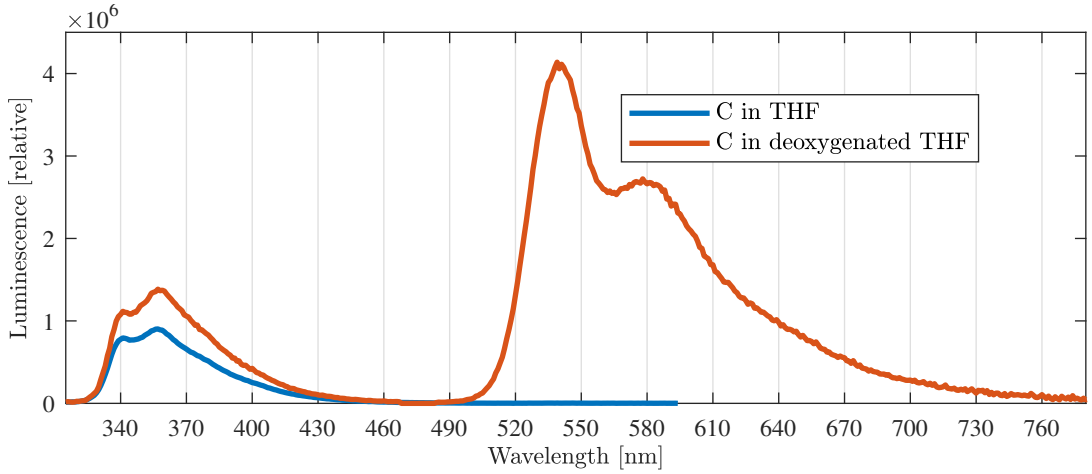

Figure 25: The figure illustates the emission spectrum of molecule C in THF and deoxygenated THF.

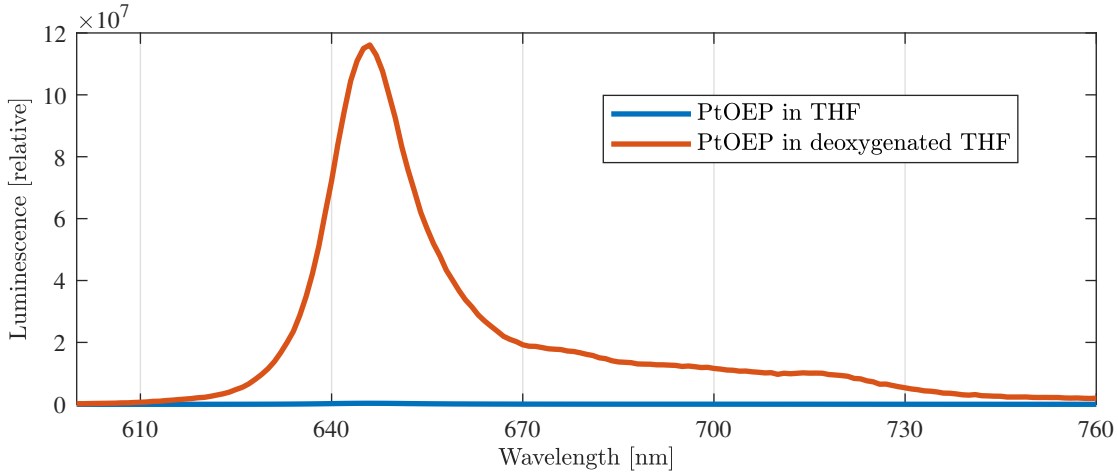

Figure 26: The figure illustates the emission spectrum of molecule PtOEP in THF and deoxygenated THF. A more zoomed in version of the same plot can be found in figure 27, to visualize the shape of the oxygenated version.

Optical power limiting abilities are apparent in molecule A, B and C from the OPL data (see figure 34 on page 40 and figures 37-66 in the appendix). As presented in the theory section, these

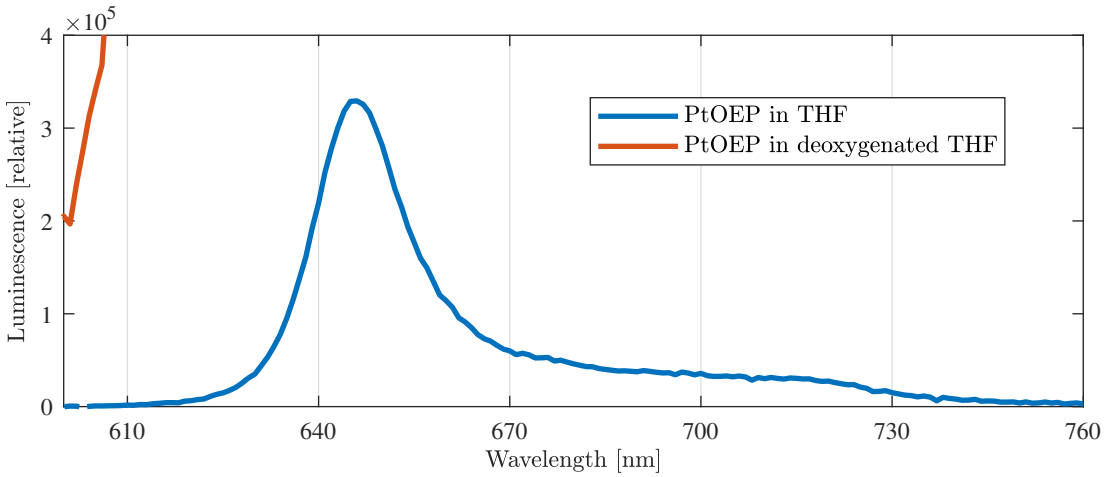

Figure 27: The figure illustates the emission spectrum of molecule PtOEP in THF and deoxygenated THF. A more zoomed out version of the same plot can be found in figure 26, to visualize the shape of the deoxygenated version.

Molecule	Solvent	n_D[a]	λ_{ex}[b]	QY
A	Tetrahydrofuran	1.407[22]	300	0.66±0.075
A	Deoxygenated tetrahydrofuran[c]	1.407[22]	300	0.70±0.15
B	Tetrahydrofuran	1.407[22]	300	0.044±0.012
B	Deoxygenated tetrahydrofuran[c]	1.407[22]	300	0.083±0.019
C	Tetrahydrofuran	1.407[22]	300	0.040±0.0031
C	Deoxygenated tetrahydrofuran[c]	1.407[22]	300	0.34±0.14
PtOEP	Tetrahydrofuran	1.407[22]	355	0.0011±0.000093
PtOEP	Deoxygenated tetrahydrofuran[c]	1.407[22]	355	0.39±0.032

[a] Refractive index of the solvent.
[b] Excitation wavelength (nm) used to make emission spectrum.
[c] Bubbled with argon for 8 minutes before measurements

Table 2: The table contains results and physical properties related to the QY.

abilities may occur from triplet state RSA, singlet state RSA and TPA. For all the molecules, the TPA/RSA ratio is so far not clear. Measuring the TPA cross section would have clarified the ratio, and this is suggested done in further studies of the molecules.

The large increase in luminescence and change of spectrum shape, when oxygen is removed, indicates that there is large excitation to the triplet states from the ground state for C and PtOEP, but little to none with A and B. This is supported by the lifetime measurements seen in table 3 on the following page, which only yielded phosphorescence lifetimes for C and PtOEP, and fluorescent lifetimes for A and B.

To further understand the characteristics of the molecules, ESA spectrum and lifetime measurements were made. Although, as explained in section 11 on page 20, there is a step in the production of the ESA spectrum where the ground state depletion A_{depl} have to be "guessed" and that percentage of the GSA A_g has to be added to the recorded OMA spectrum. As A_{depl} is solely "guessed" on the basis of removing any negative counts and making it seem sensibly aligned with the rest of the spectrum, this yield a large uncertainty in whether the ESA spectra end up as correct. In figure 30-31 the addition of different percentages are illustrated for the

Molecule	Solvent	λ_{ex} [a]	τ_f [b]	τ_p [c]	λ_{ESAmes} [d]	τ_{ESA} [e]
A	Tetrahydrofuran	300	0.79±0.012	N/A	650	0.805
A	Deoxygenated tetrahydrofuran[f]	300	N/A	N/A	650	266
B	Tetrahydrofuran	300	0.73±0.026	N/A	650	1.01
B	Deoxygenated tetrahydrofuran[f]	300	N/A	N/A	650	69
C	Tetrahydrofuran	300	N/A	N/A	650	0.807
C	Deoxygenated tetrahydrofuran[f]	300	N/A	62±0.099	650	86
PtOEP	Tetrahydrofuran	355	N/A	N/A	420	0.602
PtOEP	Deoxygenated tetrahydrofuran[f]	355	N/A	77±0.090	420	37

[a] Excitation wavelength (nm) used to make fluorescence and phosphorescence lifetime measurements. [b] Fluorescence lifetime (µs). [c] Phosphorescence lifetime (µs).
[d] Measurement wavelength (nm) used in ESA lifetime measurements. [e] ESA lifetime (µs).
[f] Bubbled with argon for 8 minutes pre-measurements.

Table 3: The table contains the lifetime measurements made in this thesis. N/A indicates an unsuccessful attempt at measuring the fluorescence/phosphorescence lifetimes.

molecules.

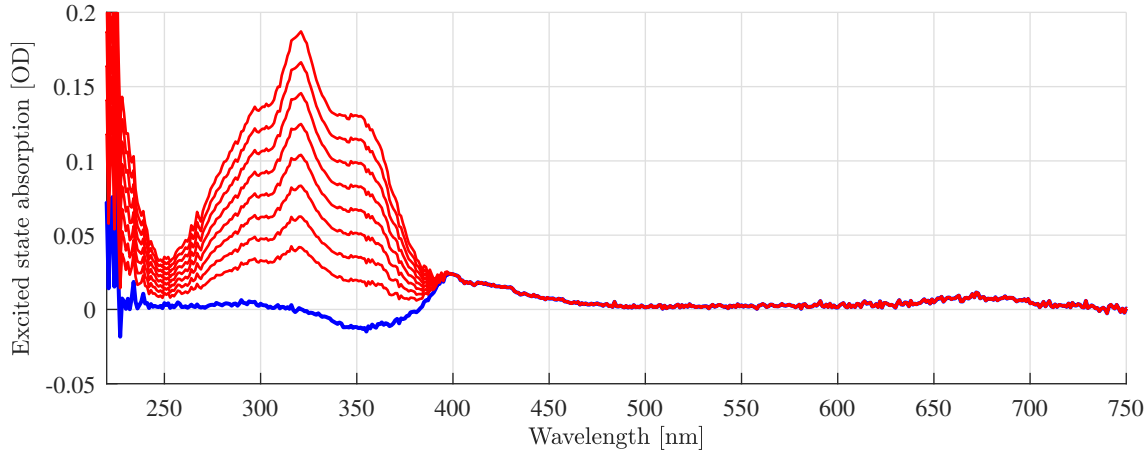

Figure 28: The figure illustrates the addition of 20%A_g to 90%A_g, with 10% intervals, to the OMA spectrum (blue) of molecule A. The molecule was excited from the ground state at 355 nm.

For all percentages added to the OMA spectrum of A, a minor dip around 370 nm-390 nm can be seen. This is the edge of the area where the absorption spectrum is added. Ignoring this dip and aligning the OMA spectrum with the ESA spectrum below 370 nm yields a percentage of about 40%(A_{depl}=0.4).

For molecule B, adding 60% seems to make a nice transition from the OMA spectrum to the ESA spectrum, in terms of keeping the second derivative of the ESA spectrum from 350 nm to 375 nm constant.

The C molecule seems to be the simplest guess, as about 70% seems to continue the spectrum from the OMA spectrum to the ESA spectrum.

Deciding the percentage for PtOEP is dependent on whether the peaks around 380 nm and 535 nm is meant to be present. As these peaks definitively originate from the addition of the GSA spectrum and as there is no link between how the shape of the GSA spectrum and the ESA

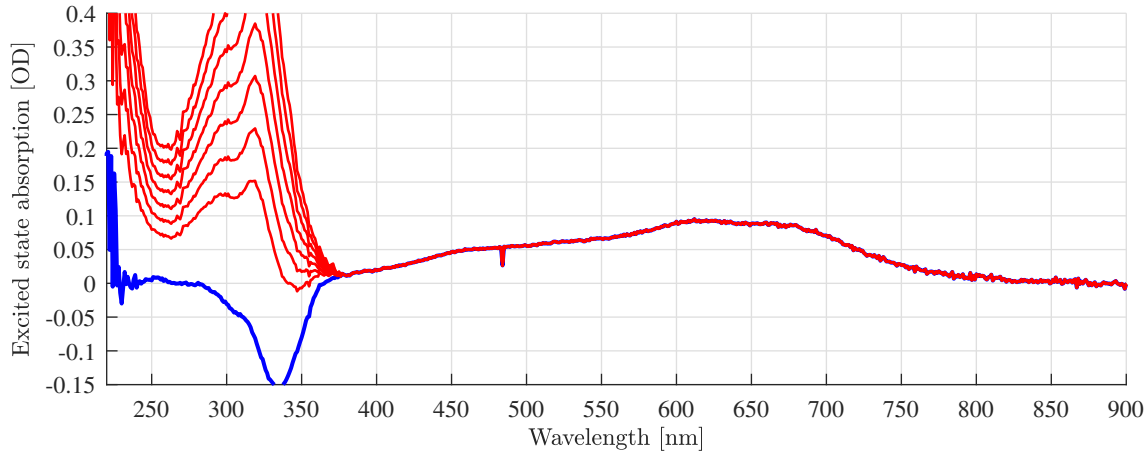

Figure 29: The figure illustrates the addition of 30%A_g to 90%A_g, with 10% intervals, to the OMA spectrum (blue) of molecule B. The molecule was excited from the ground state at 355 nm.

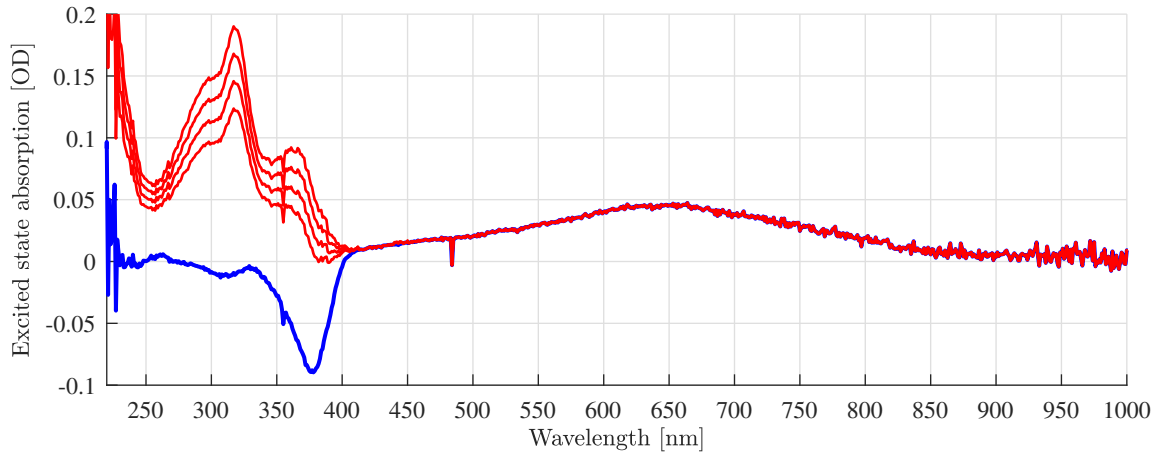

Figure 30: The figure illustrates the addition of 60%A_g to 90%A_g, with 10% intervals, to the OMA spectrum (blue) of molecule C. The molecule was excited from the ground state at 355 nm.

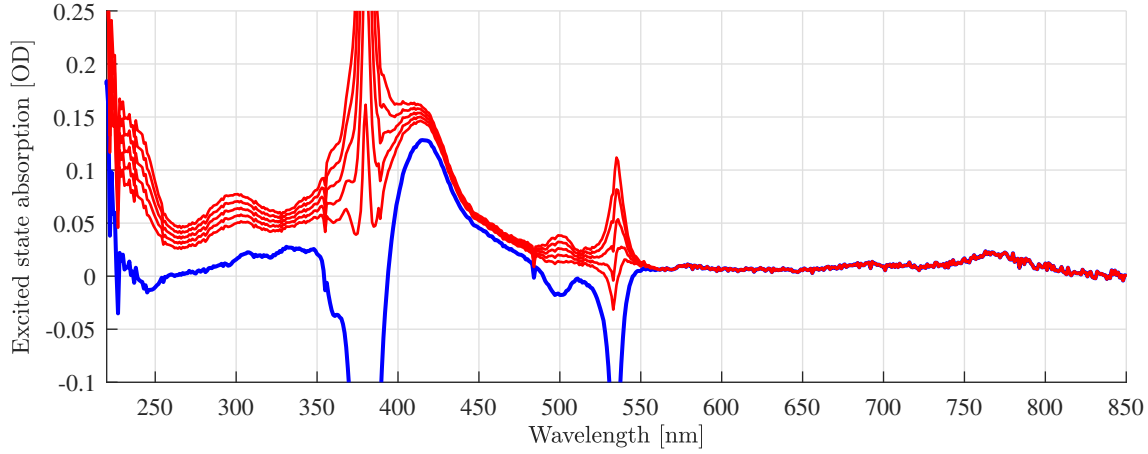

Figure 31: The figure illustrates the addition of 50%A_g to 90%A_g, with 10% intervals, to the OMA spectrum (blue) of molecule PtOEP. The molecule was excited from the ground state at 355 nm.

spectrum should look, the percentage aligning the data pre and post these peaks is chosen. The percentage for PtOEP is chosen to be 60%, and its guessed ESA spectrum can be seen in figure 32, along with the guessed spectra of the other molecules.

For A, B and C, the addition of the GSA spectra seems to mostly increase GSA spectrum peaks of the ESA spectrum. This seems to indicate that triplet absorption is not dominating in these areas. The peaks and shoulders peaks(as shown as an example in figure 32) of the areas that seems to be dominated by triplet absorption are noted in table 4 as λ_{ESAmax}. It is important to notice that the areas below the visual spectrum ($< 430\,\mathrm{nm}$) is not important for the discussion of the OPL performane.

As it is impossible to guess exactly what percentages that are correct to add, initially the range of percentages shown in the figures above will be used for further calculations. The ESA spectra can be used to calculate the ESA over GSA ratio A_{ESA}/A_g. Because of this, the ratio ranges $\Delta A_{ESA}/A_g$ based on possible depletion number ΔA_{delp} is calculated and the ratio A_{ESA}/A_g based on a guessed percentage A_{delp} is calculated. Both results can be found in table 4.

Molecule[a]	λ_{ESAmax}[b]	ΔA_{delp}[c]	$\Delta A_{ESA}/A_g$	A_{delp}	A_{ESA}/A_g
A	$400(672)$	0.2-0.99	0.63-1.42	0.4	0.83
B	$612(455)(680)$	0.3-0.99	0.70-1.39	0.6	1.00
C	653	0.6-0.99	1.35-1.75	0.70	1.46
PtOEP	$414(719)$[c]	0.5-0.99	0.63-1.12	0.6	0.73

[a] All the molecules were soluted in deoxygenated tetrahydrofuran(THF).
[b] Peak/shoulder peak wavelengths [nm]. Secondary peaks are in parenthesis. [c] The false peaks originating from the GSA are ignored.

Table 4: The data related to the produced ESA spectra.

Looking at the ESA measurements in figure 32 all, there appears some ESA in in the whole visual spectrum in comparison to the ground absorption spectra. Measuring the ESA lifetime at these new ranges produces $\sim$ µs lifetimes for all molecules (see table 3).

To better understand the mechanisms contributing to the OPL performances of the molecules (see section 2.2.4 on page 23), it is desired to check whether the molecules had any transition from the ground state to the first triplet state (the forbidden transition $\sigma(S_0T_1)$). This transition should in theory be seen as a part of the absorption plot, but as the cross section of the transition usually is very small, it can not be seen. As the transition is to the triplet state it contributes to the phosphorescence of the molecule. If the phosphorescence parts of the molecules emission spectrum can be located, an excitation scan with the measurement wavelength in this range might show the location and size of forbidden transition absorption. This was done for C, as it were the only molecule displaying a separate phosphorescence range (see figure 25). Using a $640\,\mathrm{nm}$ measurement wavelength, a new absorption peak was found. This new absorption peak is shown in figure 33, and by dividing the integral of the forbidden transition peak with the integral of the whole spectrum, the percentagewise contribution of the forbidden transition to the triplet state, per total transition contribution to the triplet state, can be estimated. The contribution was found to be approximately 1%.

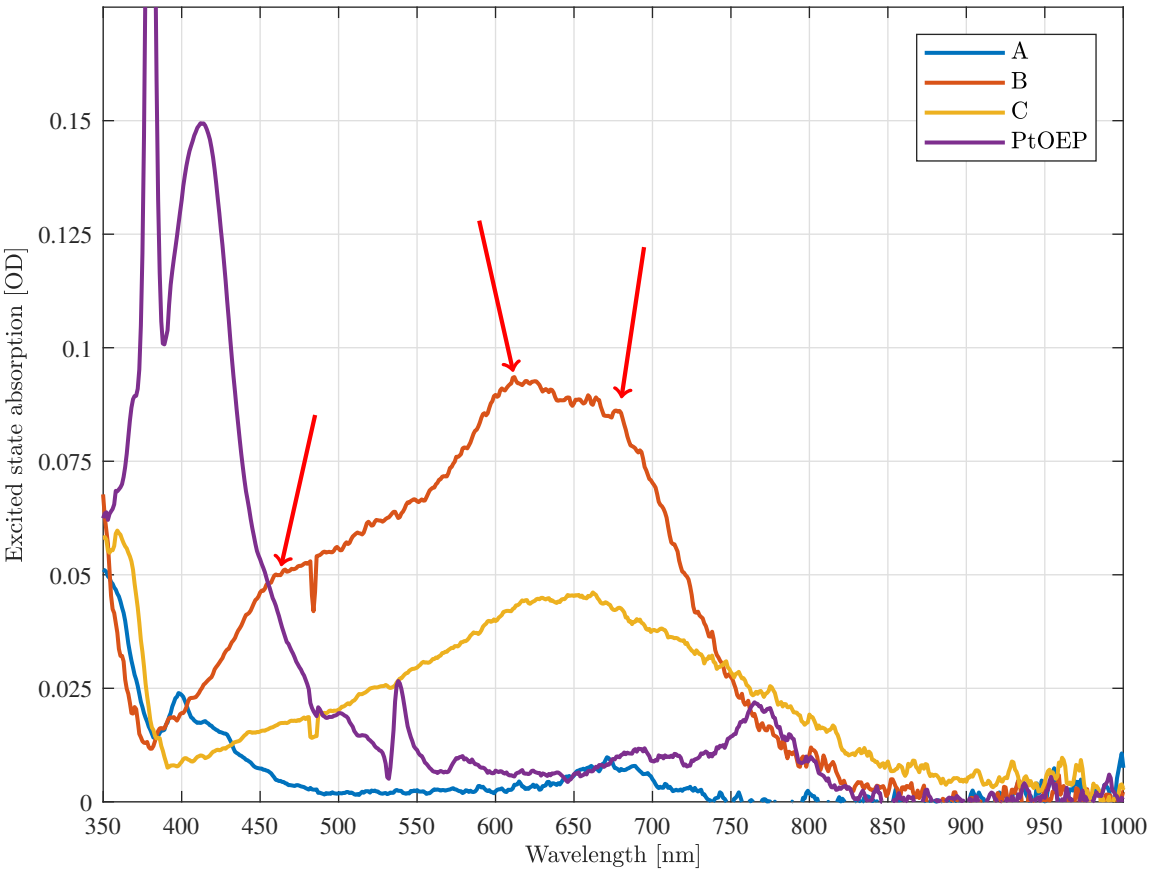

Figure 32: The figure is a plot of the guessed ESA absorption spectra data. As an example, the peaks and shoulder peaks of molecule B are indicated by red arrows. The full spectrum can by seen in figure 36 in the appendix.

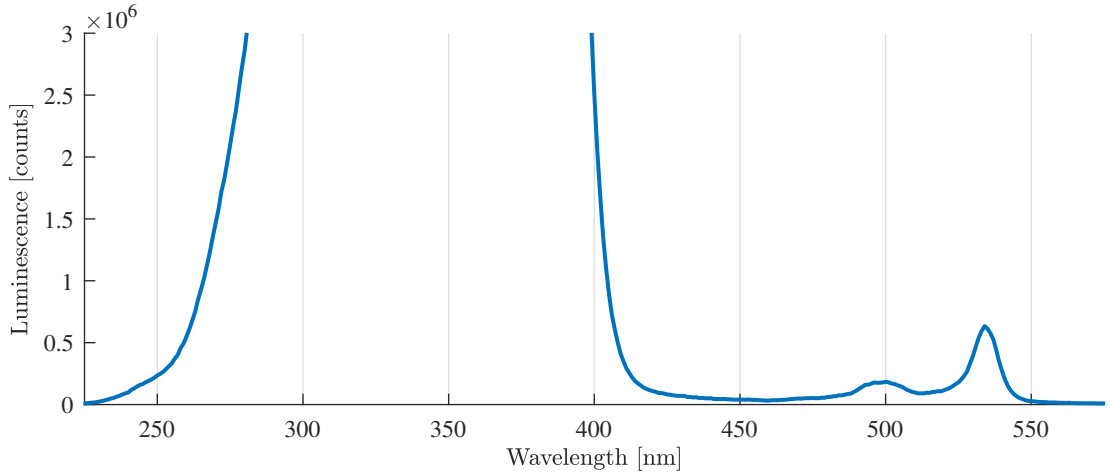

Figure 33: The figure illustrates the a zoomed in version of the excitation spectrum of C, clearly showing forbidden triplet state absorption around $490\,\text{nm} - 550\,\text{nm}$, with two peaks at $500\,\text{nm}$ and $534\,\text{nm}$. The measurement wavelength is $640\,\text{nm}$.

3.7 Phothysical measurements in light of the OPL data

A general point about the measurements is that molecule A, B and C seem to have zero absorption (except for the forbidden transition of C) in the visual spectrum (the same wavelength range

that the OPL measurements are made in), implying that there can be none RSA, as no electrons are excited to a higher state in the first place. This makes the case that the OPL performance only originates from TPA, as half the wavelength (double the energy) of the whole spectrum has GSA. However, this is probably not the case, as there always are some GSA and as TPA actually can contribute to RSA by absorption to singlet or triplet states. As all three molecules have some ESA in the visual area, just a little absorption would make all the molecules reverse saturable absorbers (RSA). This is why potentially measuring the TPA spectra in further studies will be very useful in order to understand more of the detailed mechanisms.

Combining the ESA data, excitation spectrum data, emission spectrum data and the lifetime measurements. Some indications of what sort of contributions to the OPL performance (see figure 34) the different RSA and TPA mechanisms have, are made in this section. Even do figure 34 only represent a single value (averaged over five data points) for each wavelength (at input fluence $25\,\mathrm{J/cm^2}$), these values are all in the second linear area of the OPL data plots (see section B in the appendix), thus giving a good representation of the OPL performance.

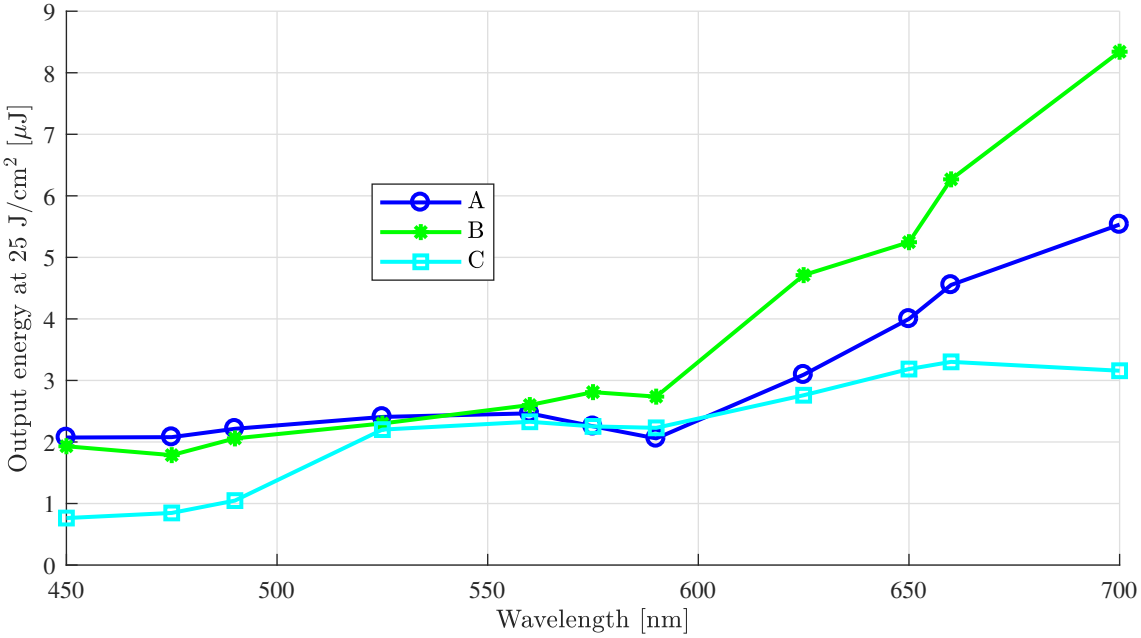

Figure 34: The plot visualizes the output energies at all of the measured wavelengths at a specific input energy ($25\,\mathrm{J/cm^2}$) for A, B and C (averaged over five data points). Molecule C seems to inhabit the best OPL performance overall. $< 525\,\mathrm{nm}$ C has twice the nonlinear effect of A and B. $525\,\mathrm{nm} \leq 590\,\mathrm{nm}$ all three molecules are approximately the same, as C is raised to the same level of A and B. $> 590\,\mathrm{nm}$ the nonlinear effect seems to decline for all three molecules. Where B declines the most, following A and then C.

First of, noticing that the molecule scoring the overall best on the OPL measurement is C, it is natural to investigate how C differs from A and B in the other measurements. The difference is, however, mainly in the upper and lower part of the visual spectrum. Attributing this performance to C having most contribution from triplet RSA, out of the three molecules, does, initially, not seem correct as B has a larger ESA cross section $\sigma_{T_1T_N}$ for all wavelengths in the visual spectrum (seen in figure 35). But, the emission spectra makes it clear that C clearly has the most inter-system system crossing out of A, B and C. By looking at the relative sizes of the two emission peak integrals of molecule C in figure 25 on page 34, the ISC seem to be at about

85%, only beaten by PtOEP with ∼100% ISC (confirmed by Bansal et.al. [5]). This suggest that there is more GSA to the triplet states for C, than for A and B, resulting in more triplet RSA for C, than for A and B, heightening the OPL performance of C.

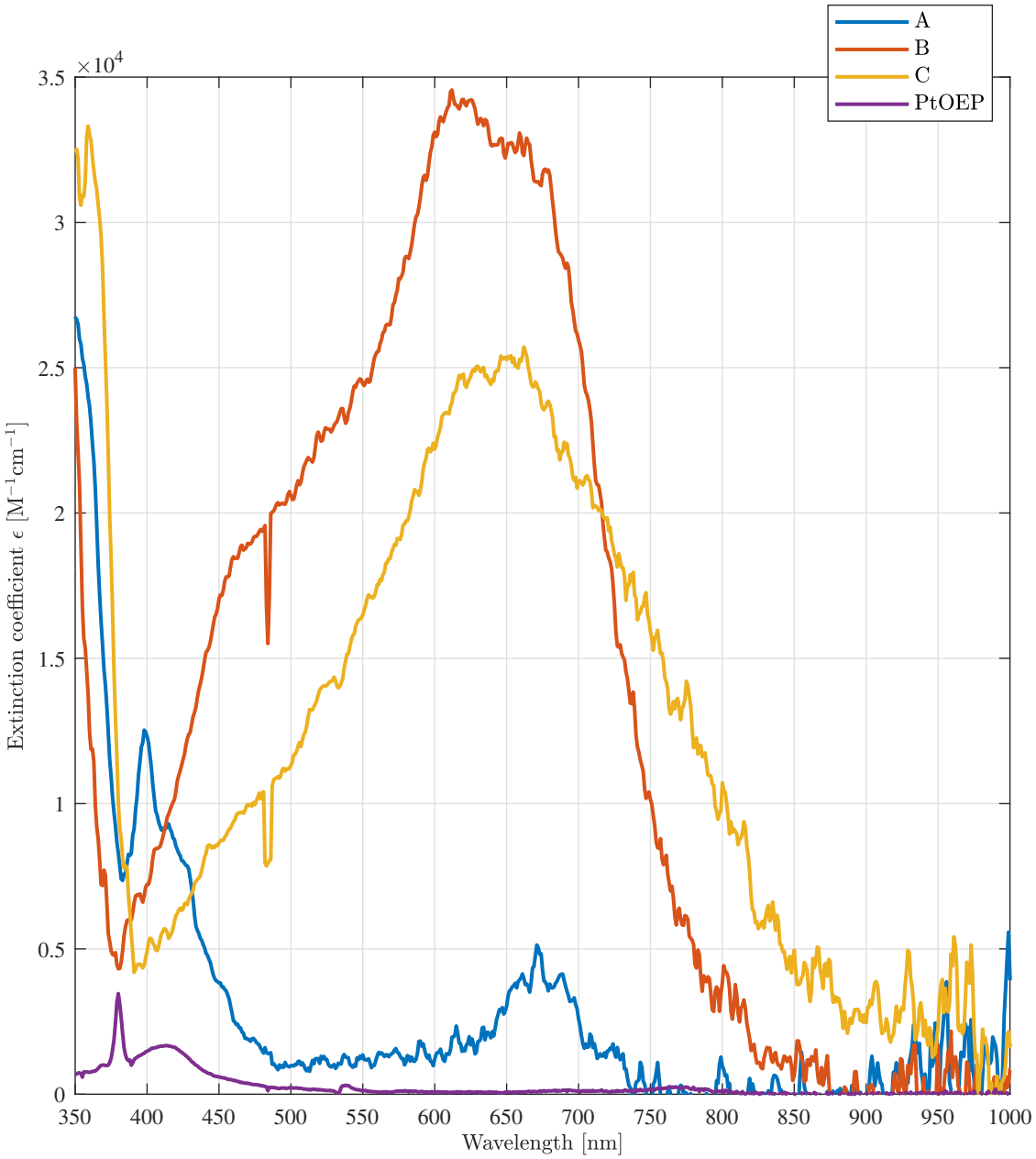

Figure 35: The figure illustrates the plotted data of triplet state extinction coefficient $\epsilon_{T_1T_N}$.

Glimsdal models 10% and 20% forbidden absorption (percentage of ESA $\epsilon = 10^{-4}[\mathrm{M}^{-1}\mathrm{cm}^{-1}]$) and the increase in OPL performance was raised by around 66% to 100%[4]. Looking at the relative sizes of the forbidden transition spectrum and the rest of the excitation scan absorption spectrum of C (see in figure 33), and looking at the relative sizes of the excitation scan absorption spectrum and the extinction coefficient spectrum of C. Rough estimations sets the extinction coefficient of the forbidden absorption to about 5%-10% of the extinction coefficient of C. As this forbidden transition was only measured in the lower ranges of the visible spectrum, it seems to be a clear contributor to the OPL performance of C at those wavelength.

Another point about the high OPL performance of C in the lower wavelengths, is that C is

the molecule with the absorption spectrum stretching furthest into the visible spectrum (see figure 33 on page 39), potentially being a factor that helps doubling the performance of C in relation to A and B. It seems that the main mechanisms behind the OPL performance of C is one photon absorption (triplet RSA) at the lowest wavelengths, gradually overlapping with the forbidden transition (triplet RSA).

A and B performs almost equally (in terms of OPL) up to $560\,\mathrm{nm}$, but A outperforms B after that. As no GSA to the triplet states or forbidden transition has been found for these molecules, there is no indications of triplet RSA playing any leading role in the OPL performance of either A or B, unless there excists undiscovered forbidden transitions $\sigma_{S_0T_1}$ or TPA to the triplet state. As B have about a ten times larger ESA extinction coefficient than A, it is likely that an increased TPA to the triplet states, TPA by it self or singlet RSA, is causing A to outperform B. A rather large difference between A and B is the quantum yields as seen in table 2 on page 35, may be a contributing factor to the singlet RSA. Again, doing the TPA measurements would help with unveiling the contribution from the different mechanisms.

In trying to estimate how well PtOEP would have done in OPL measurements, the first thing that is clear, is that none of the OPL performance can be caused by singlet RSA, as the molecule have a $\sim 100\%$ ISC. By looking at the exctinction coefficient spectrum at page three, PtOEP is the only molecule with any measurable amount of absorption in the visible spectrum. This might contribute some to its triplet RSA, but as PtOEP has a very low triplet state extinction coefficient $\sigma_{T_1T_N}$ in the visual spectrum, in comparison to the other molecules, the triplet RSA will be low. As $\sigma_{T_1T_N} < \sigma_{S_0T_1}$ in parts of the lower visible spectrum, the molecule will actually be a SA, obstructing the OPL performance. If PtOEP should have OPL performance in the magnitudes of A, B and C, it would have to mainly arise from TPA.

The ESA lifetime are for all the molecules significantly longer than the pulse length of the system, keeping any excited electrons excited during the whole beam length. This would however had affected the OPL performance of a continuous wave, as A potentially could keep the electrons in an excited triplet state three to seven times longer than the other molecules (see table 3 on page 36). Whether this would be the case is uncertain as A seems to have little or none absorption to the triplet states by the lack of ISC, and is dependent on potential discoveries of forbidden transition $\sigma_{S_0T_1}$ or TPA ω_S to the triplet states.

It is also important to notice that the size of the ESA extinction coefficients are inversely proportional to the chosen A_{depl} values. Their relative size could be somewhat off, potentially invalidating some of the discussion above.

Another point that should be made in regards to the comparison of the relative OPL performance of the molecules, is that the scattering effect caused by the creation of plasma bubbles may be nonlinear. More absorption will cause more bubbling, that will cause more scattering, potentially making the differences of performance larger than they initially were.

4 Conclusion

In this thesis the photophysical properties of three novel molecules A, B and C and a fourth previously well investigated molecule, PtOEP was measured. The measured data includes absorption spectra, emission spectra, extinction spectra, (triplet) excited state absorption spectra, fluorescent lifetimes, phosphorescence lifetimes and excited state absorption lifetimes in both oxygenated and deoxygenated solvent. How well the oxygen was removed from the solvent was discussed and found to be sufficiently well. A method for removing second order harmonic diffraction to produce a full emission spectrum was also discussed. Most of the results was discussed, enlightening the differences and similarities between the different molecules.

Also, measurements of the optical power limiting performance (OPL) was made of molecule A, B and C. The detection of some "jumps" in the plotted results was explained by the changing of the input range of the signal detector. Devaluing the data, a problem with scattering due to the production of plasma bubbles at high fluences was discussed, resulting in scattering representing a part of the non-linearity/OPL performance of the data. An imaginary example of using the three molecules in actual OPL filters, protecting a specific optical system against a specific incident pulsed laser beam was illustrated and discussed, based on the measured OPL performances. At the specific laser beam wavelength $450\,\mathrm{nm}$, the damage threshold of the C-filter could protect an optical system with the damage threshold being 33% and 38% of the intensity to the damage threshold of an optical system protected by a A-filter and B-filter, respectively.

By combining the OPL data and the more general photophysical data, the relative contributions of the three mechanisms triplet RSA, singlet RSA and TPA to the OPL performance of A, B and C, was attempted sorted out. A finding in this thesis is that the TPA needs to be further characterized, to explain these mechanisms. However, triplet RSA seems to be a larger factor for the OPL of C than for A and B, and it is certainly contributing to the OPL abilities of C. It is also clear that for C, a forbidden transition and its wide GSA spectrum contributes to the triplet RSA at low wavelengths in the visible spectrum. Unless A and B has a forbidden transition to the triplet state or TPA to the triplet state, only TPA and singlet RSA contribute to the OPL performance. PtOEP does not have any singlet RSA, and is thought to under-perform in comparison to the other three molecules, unless it has a very high TPA.

C is the molecule with the overall best OPL performance, and it can be attributed to its high ISC, its wide GSA spectrum, its forbidden state transition and its high ESA. Molecule A may potentially perform better protecting against continuous wave laser than short ns pulses, due to its long ESA lifetime.

In further studies a search for the forbidden triplet transitions could also be done for A and B. As A, B and C are quite equal molecules, it is possible that emission from a potential S_0T_1 transition for A and B might occur at the same place as for C. Conducting multiple excitation spectrum scans with measurement wavelengths around C's triplet emission range might unveil forbidden transitions for A and B. The TPA should also be measured, to sort out the contributions to the OPL performances.

To avoid plasma bubble scattering, solvents with a higher plasma bubble formation threshold and/or a different sample spot size should be used in new OPL measurements of A, B and C. Potentially, measurements with glass samples could be done to look at the molecules in a new medium, while also avoiding the plasma bubble scattering issue.

References

[1] D. Haley and O. Pratt, "Basic principles of lasers," *Anaesthesia & Intensive Care Medicine*, 2017.

[2] C. Giuliano and L. Hess, "Nonlinear absorption of light: optical saturation of electronic transitions in organic molecules with high intensity laser radiation," *IEEE Journal of Quantum Electronics*, vol. 3, no. 8, pp. 358–367, 1967.

[3] H. Lundén, E. Glimsdal, M. Lindgren, and C. Lopes, "How to assess good candidate molecules for self-activated optical power limiting," *Optical Engineering*, vol. 57, no. 3, p. 030802, 2018.

[4] E. Glimsdal, "Spectroscopic characterization of some platinum acetylide molecules for optical power limiting applications," 2009.

[5] A.-K. Bansal, W. Holzer, A. Penzkofer, and T. Tsuboi, "Absorption and emission spectroscopic characterization of platinum-octaethyl-porphyrin (ptoep)," *Chemical physics*, vol. 330, no. 1-2, pp. 118–129, 2006.

[6] F. Nifiatis, W. Su, J. E. Haley, J. E. Slagle, and T. M. Cooper, "Comparison of the photophysical properties of a planar, ptoep, and a nonplanar, ptoetpp, porphyrin in solution and doped films," *The Journal of Physical Chemistry A*, vol. 115, no. 47, pp. 13764–13772, 2011.

[7] J. R. Lakowicz, "Introduction to fluorescence," in *Principles of fluorescence spectroscopy*, pp. 1–23, Springer, 1999.

[8] J. Clark and G. Gunawardena, "The beer-lambert law." https://chem.libretexts.org/Core/Physical_and_Theoretical_Chemistry/Spectroscopy/Electronic_Spectroscopy/Electronic_Spectroscopy_Basics/The_Beer-Lambert_Law, 2017. Accessed: 01-12-2017.

[9] "3010/3310." http://www.labequip.com/stock/pictures/30389.pdf. Accessed: 14-12-2017.

[10] "New pti quantamaster 8000 series fluorometers." http://www.horiba.com/scientific/products/fluorescence-spectroscopy/steady-state/new-pti-quantamaster-8000-series-fluorometers/. Accessed: 14-12-2017.

[11] J. R. Lakowicz, "Quenching of fluorescence," in *Principles of fluorescence spectroscopy*, pp. 257–301, Springer, 1983.

[12] H. Ramesh, T. Mayr, M. Hobisch, S. Borisov, I. Klimant, U. Krühne, and J. M. Woodley, "Measurement of oxygen transfer from air into organic solvents," *Journal of chemical technology and biotechnology*, vol. 91, no. 3, pp. 832–836, 2016.

[13] "A guide to recording fluorescence quantum yields." http://www.horiba.com/fileadmin/uploads/Scientific/Documents/Fluorescence/quantumyieldstrad.pdf. Accessed: 14-12-2017.

[14] L. W. Tutt and T. F. Boggess, "A review of optical limiting mechanisms and devices using organics, fullerenes, semiconductors and other materials," *Progress in quantum electronics*, vol. 17, no. 4, pp. 299–338, 1993.

[15] E. Glimsdal, I. Dragland, M. Carlsson, B. Eliasson, T. B. Melø, and M. Lindgren, "Triplet excited states of some thiophene and triazole substituted platinum (ii) acetylide chromophores," *The Journal of Physical Chemistry A*, vol. 113, no. 14, pp. 3311–3320, 2009.

[16] M. Sheik-Bahae, A. A. Said, T.-H. Wei, D. J. Hagan, and E. W. Van Stryland, "Sensitive measurement of optical nonlinearities using a single beam," *IEEE journal of quantum electronics*, vol. 26, no. 4, pp. 760–769, 1990.

[17] T. McKay, J. Staromlynska, J. Davy, and J. Bolger, "Cross sections for excited-state absorption in a pt: ethynyl complex," *JOSA B*, vol. 18, no. 3, pp. 358–362, 2001.

[18] D. James and K. McEwan, "Bubble and refractlve processes ln carbon suspenslons," in *Proceedings of [the] First International Workshop on Optical Power Limiting: Cannes, France, 28 June-1 July 1998*, vol. 21, p. 377, CRC Press, 1999.

[19] J. Staromlynska, T. McKay, and P. Wilson, "Broadband optical limiting based on excited state absorption in pt: ethynyl," *Journal of Applied Physics*, vol. 88, no. 4, pp. 1726–1732, 2000.

[20] M. J. Miller, A. G. Mott, and B. P. Ketchel, "General optical limiting requirements," in *Nonlinear Optical Liquids for Power Limiting and Imaging*, vol. 3472, pp. 24–30, International Society for Optics and Photonics, 1998.

[21] D. Chateau, F. Chaput, C. Lopes, M. Lindgren, C. Brannlund, J. Ohgren, N. Djourelov, P. Nedelec, C. Desroches, B. Eliasson, *et al.*, "Silica hybrid sol–gel materials with unusually high concentration of pt–organic molecular guests: Studies of luminescence and nonlinear absorption of light," *ACS applied materials & interfaces*, vol. 4, no. 5, pp. 2369–2377, 2012.

[22] "Tetrahydrofuran." https://www.sigmaaldrich.com/chemistry/solvents/tetrahydrofuran-center.html. Accessed: 06-11-2017.

A Full ESA spectra

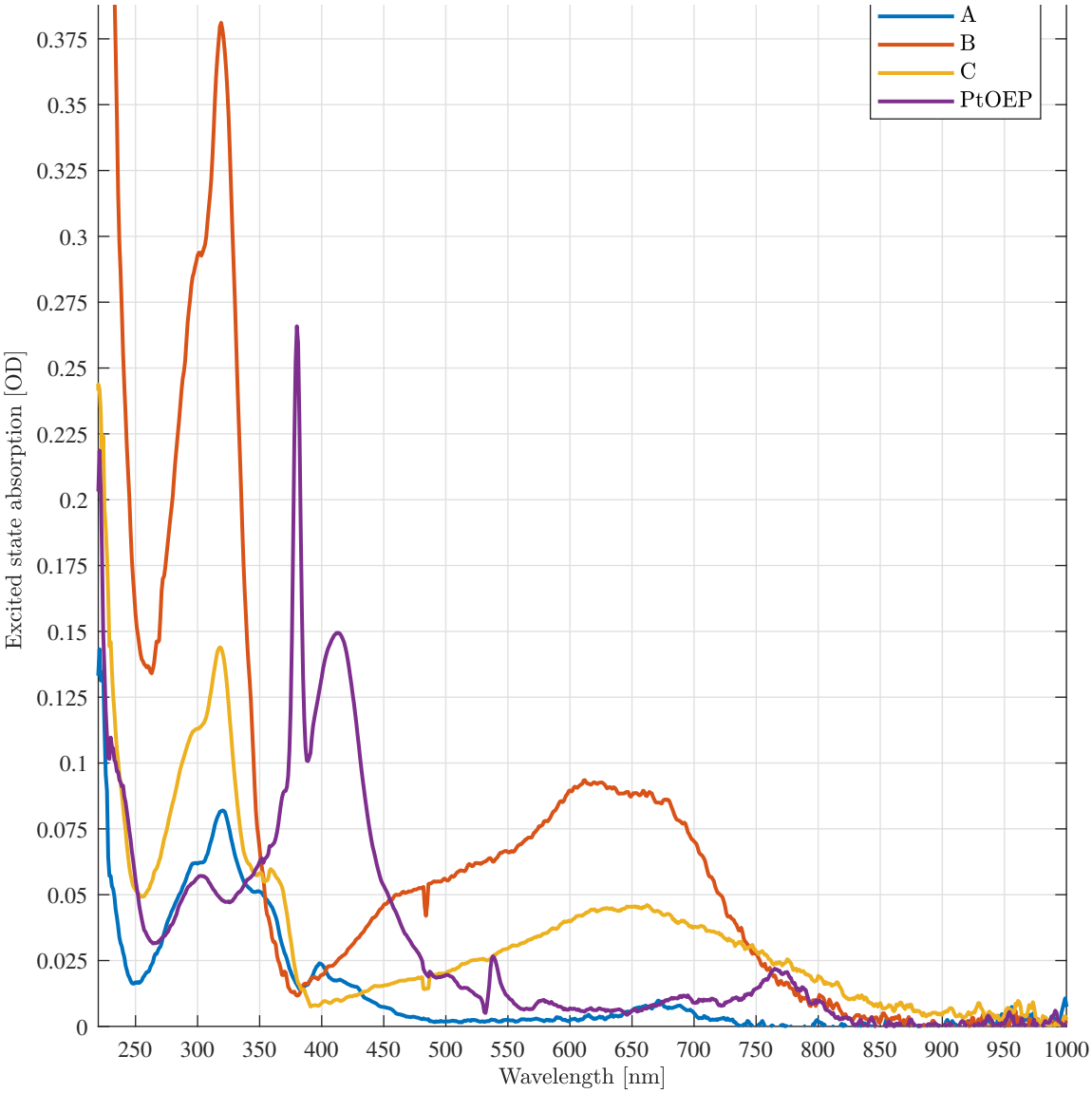

Figure 36: The figure illustrates the full ESA spectrum of all the molecules.

B OPL data plots

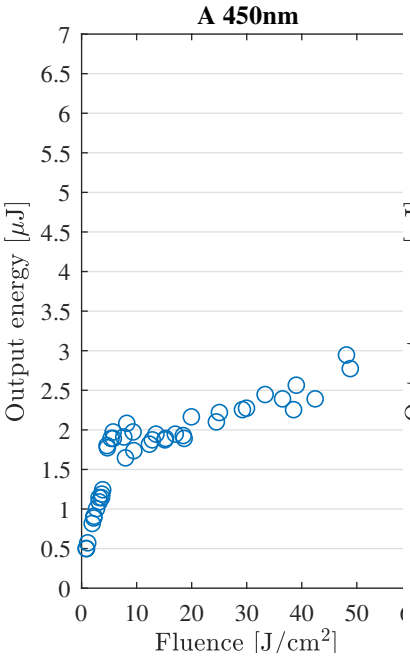

Figure 37: A figure

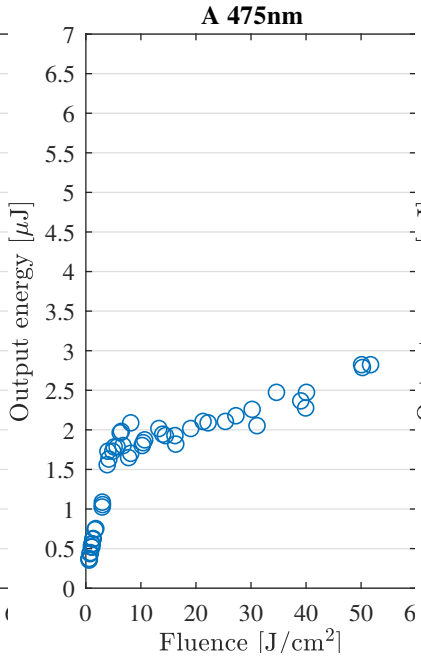

Figure 38: Another figure

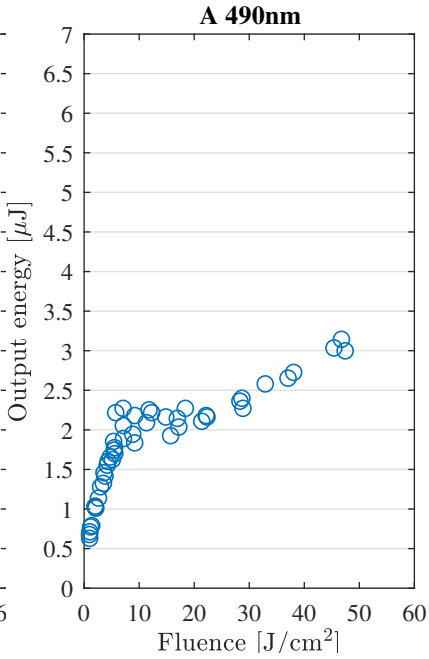

Figure 39: Another figure

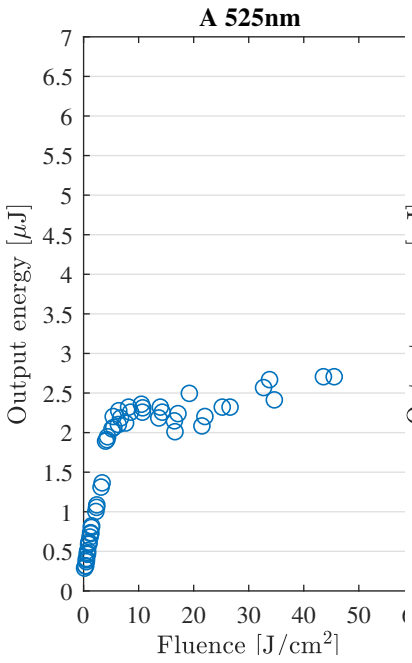

Figure 40: A figure

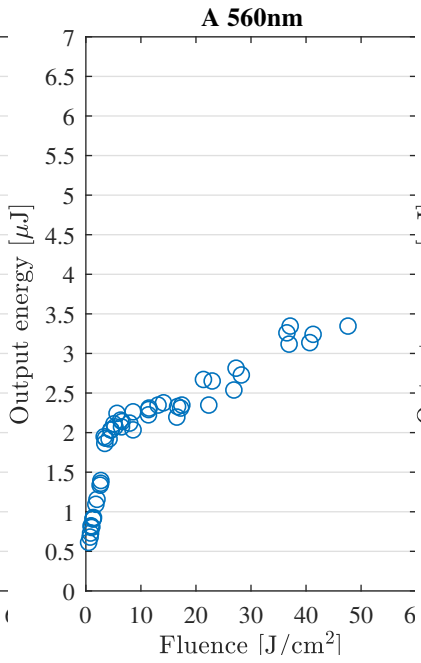

Figure 41: Another figure

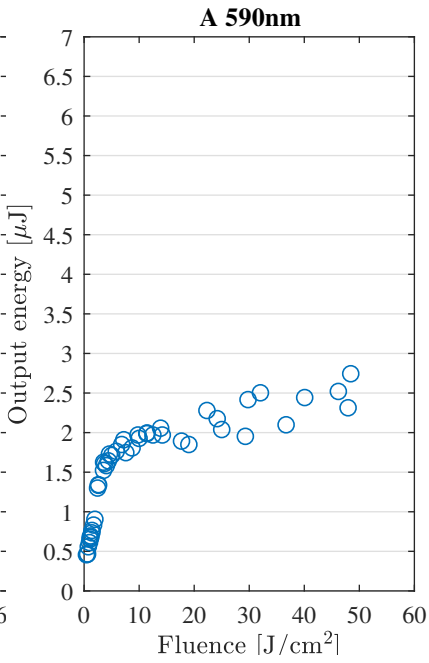

Figure 42: Another figure

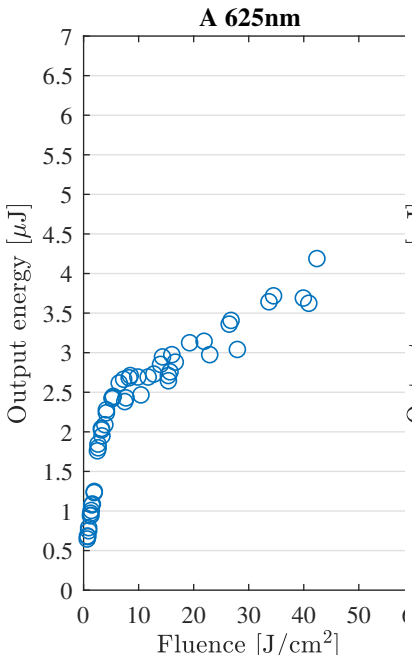

Figure 43: A figure

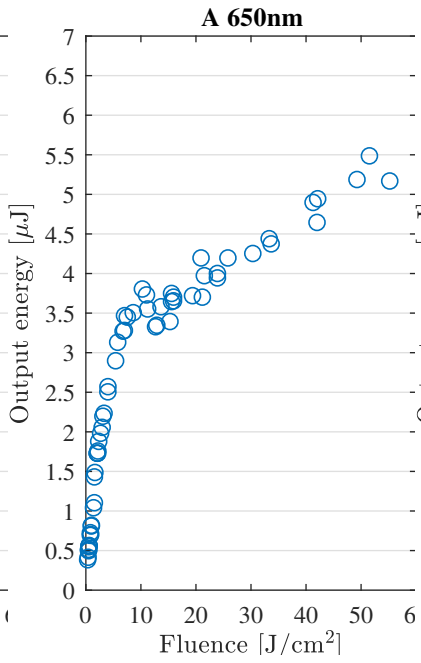

Figure 44: Another figure

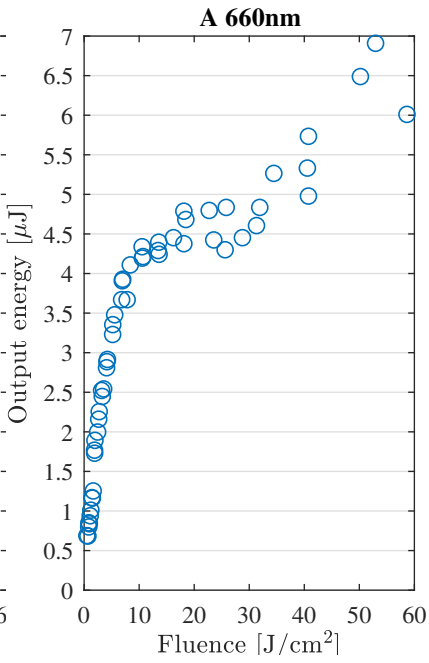

Figure 45: Another figure

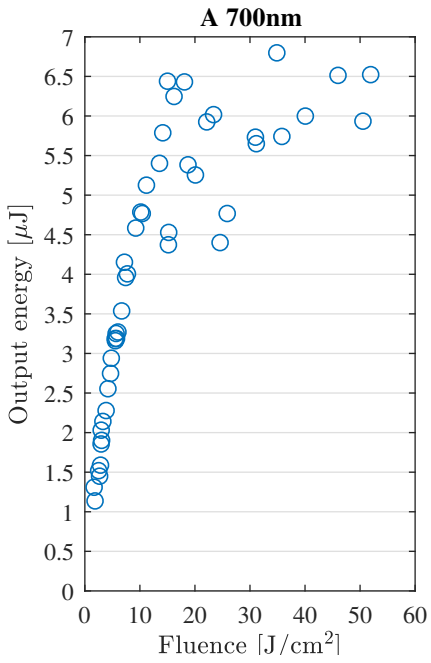

Figure 46: A figure

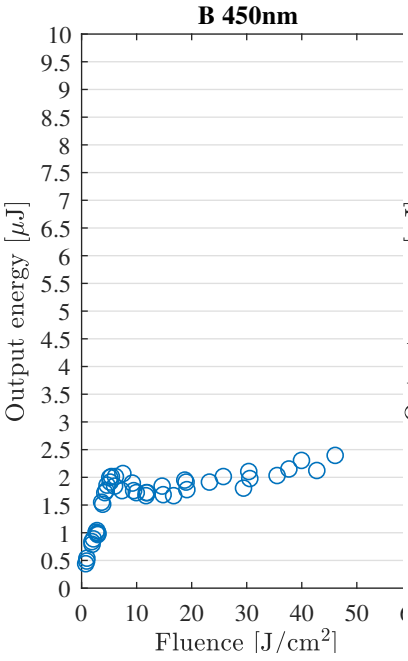

Figure 47: A figure

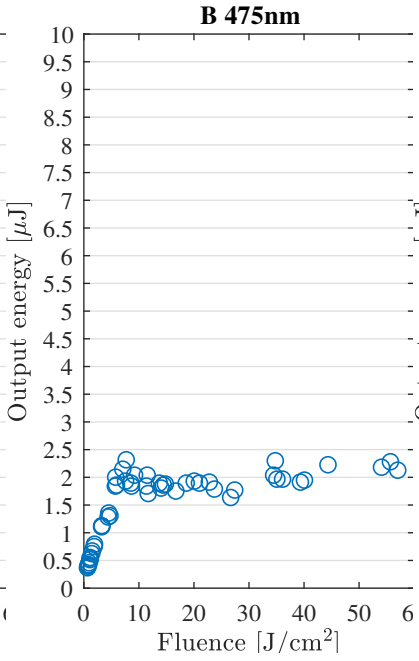

Figure 48: Another figure

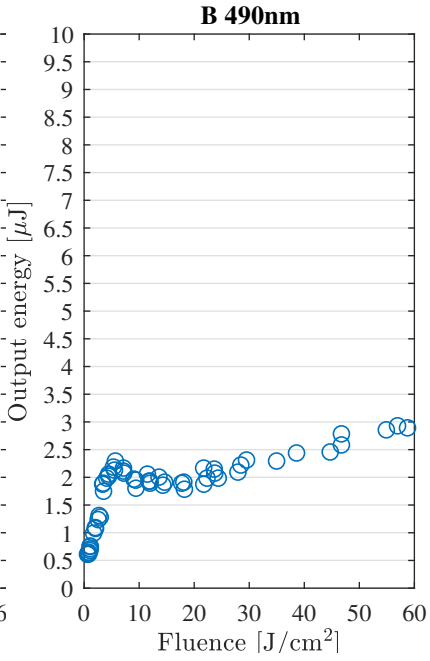

Figure 49: Another figure

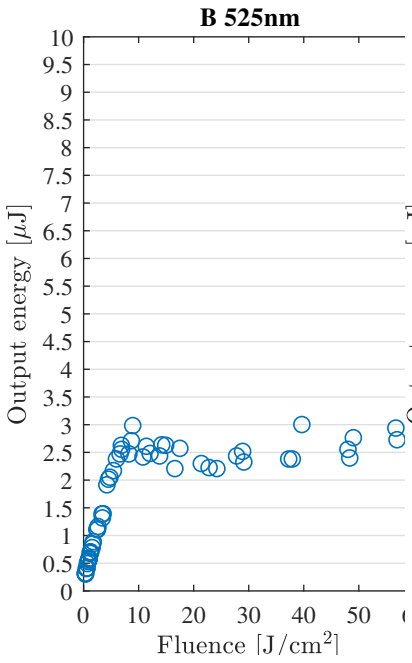

Figure 50: A figure

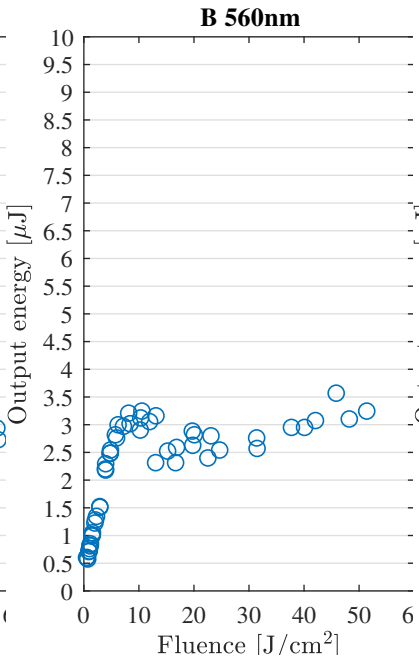

Figure 51: Another figure

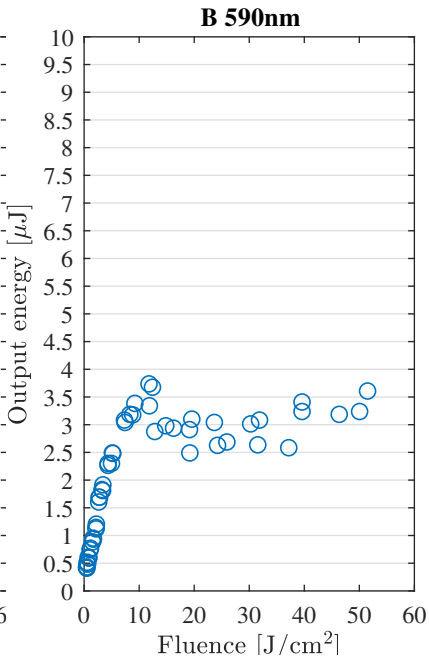

Figure 52: Another figure

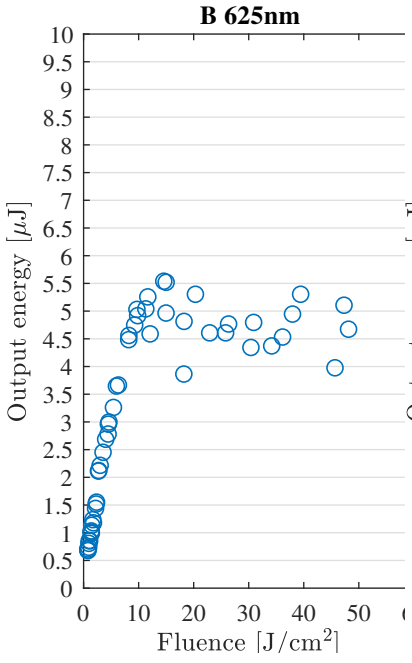

Figure 53: A figure

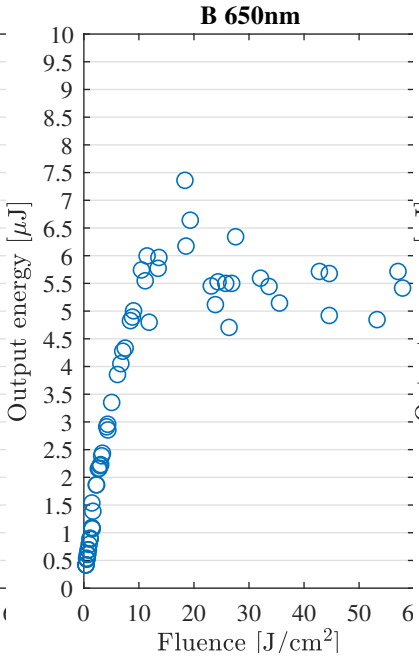

Figure 54: Another figure

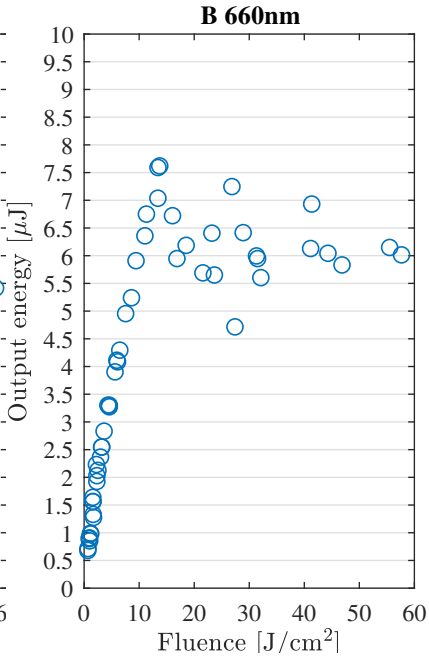

Figure 55: Another figure

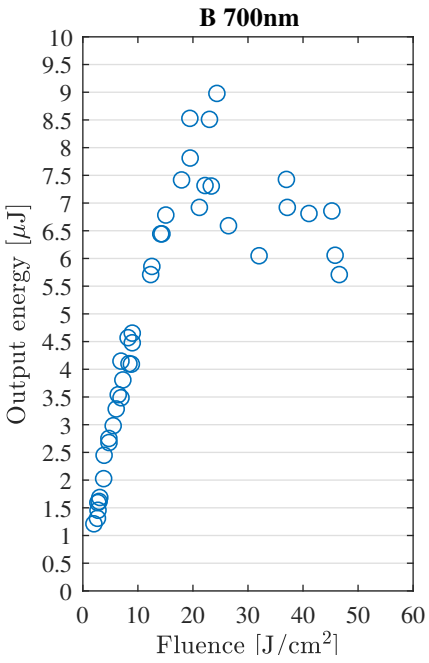

Figure 56: A figure

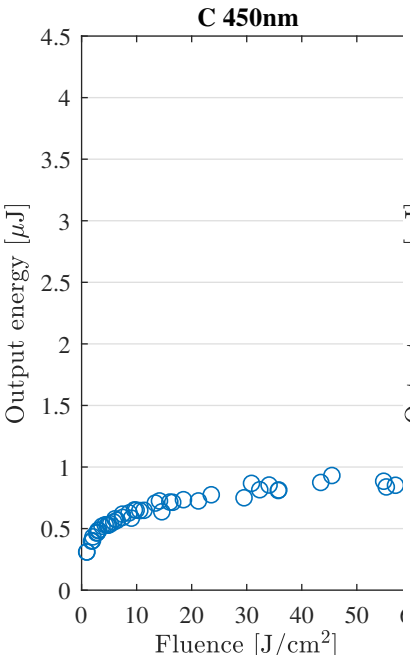

Figure 57: A figure

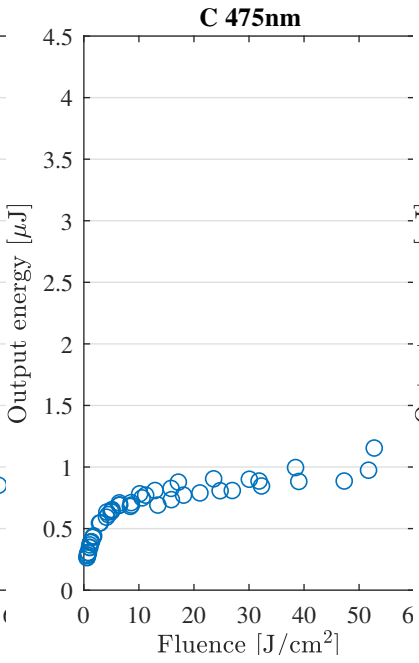

Figure 58: Another figure

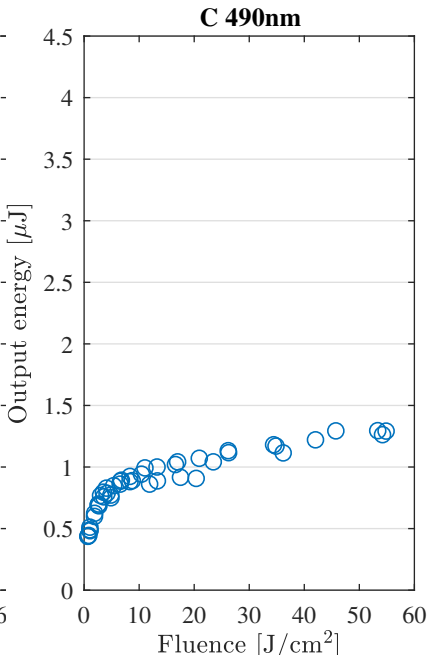

Figure 59: Another figure

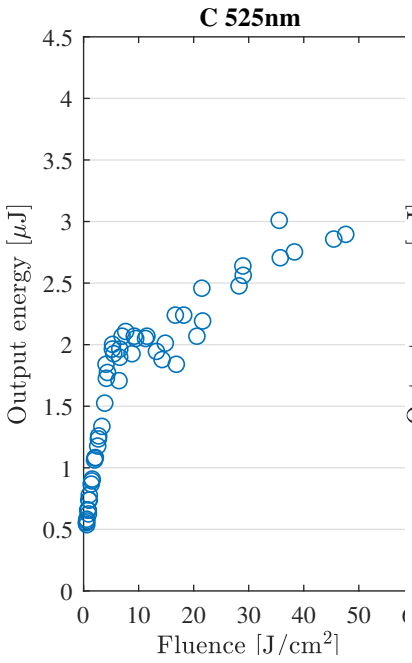

Figure 60: A figure

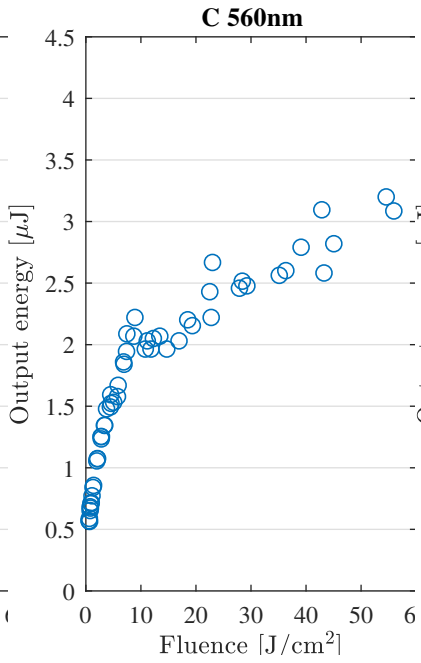

Figure 61: Another figure

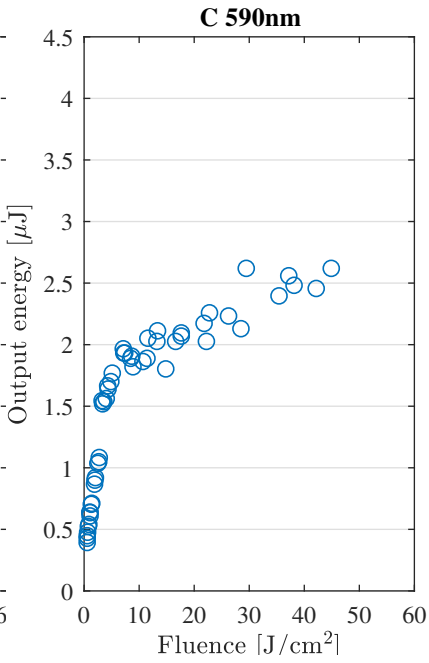

Figure 62: Another figure

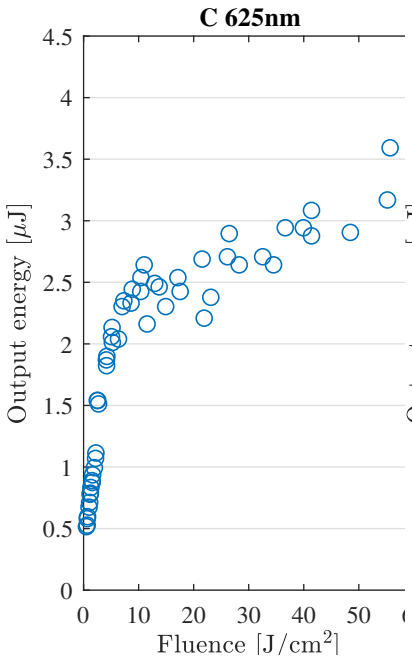

Figure 63: A figure

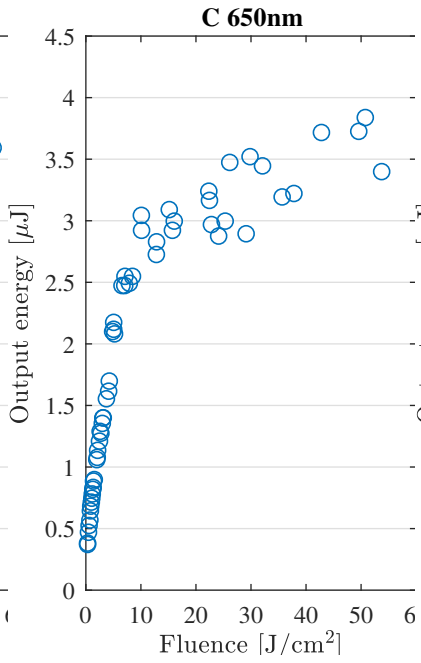

Figure 64: Another figure

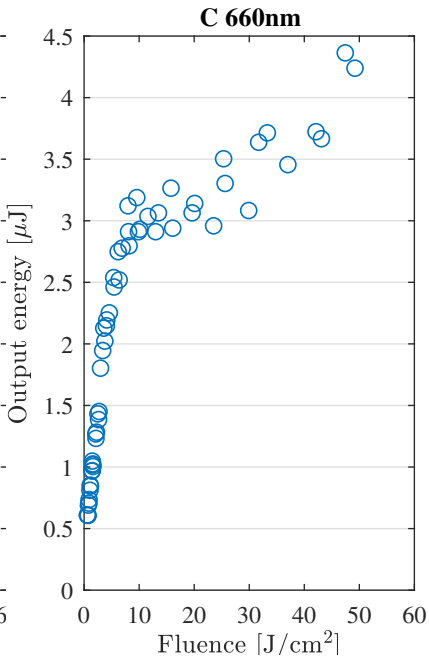

Figure 65: Another figure

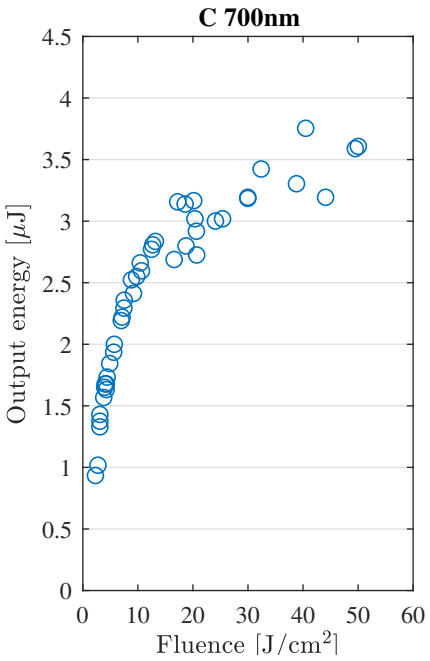

Figure 66: A figure